ORIGINAL PAPER

Niche separation between different functional types of mixoplankton: results from NPZ-style N-based model simulations

Anna-A Anschütz[1,2,3] · Kevin J. Flynn[1]

Abstract

Protist plankton comprise phytoplankton (incapable of phagotrophy), protozooplankton (incapable of phototrophy) and mixoplankton (capable of phototrophy and phagotrophy). Of these, only phytoplankton and zooplankton are typically described in models. Over the last decade, however, the importance of mixoplankton across all marine biomes has risen to prominence. We thus need descriptions of mixoplankton within marine models. Here we present a simple yet flexible N-based model describing any one of the five basic patterns of protist plankton: phytoplankton, protozooplankton, and the three functional groups of mixoplankton: general non-constitutive mixoplankton (GNCM), specialist non-constitutive mixoplankton (SNCM), and constitutive mixoplankton (CM). By manipulation of a few input switch values, the same model can be used to describe any of these patterns, while adjustment of salient features, such as the percent of C-fixation required for mixotrophic growth, and the rate of phototrophic prey ingestion required to enable growth of GNCM and SNCM types, readily provides fine tuning. Example outputs are presented showing how the performance of these different protist configurations accords with expectations (set against empirical evidence). Simulations demonstrate clear niche separations between these protist functional groups according to nutrient, prey and light resource availabilities. This addition to classic NPZ plankton models provides for the exploration of the implications of mixoplankton activity in a simple yet robust fashion.

Introduction

Although often superseded by variable stoichiometric constructs, the simplicity of the classic nitrogen-based NPZ model (Fasham et al. 1990; Franks 2002) still finds favour as a tool for exploration of conceptual ecology, and also in

✉ Kevin J. Flynn
  k.j.flynn@swansea.ac.uk; kjfplankton@gmail.com

[1] Biosciences, Swansea University, Singleton Park, Swansea SA2 8PP, UK

[2] School of Earth and Ocean Sciences, Cardiff University, Park Place, Cardiff, Wales CF10 3AT, UK

[3] Université libre de Bruxelles, Ecologie des Systémes Aquatiques, cp-221, Boulevard du Triomphe, 1050 Brussels, Belgium

large-scale models where computational costs are at a premium (Yool et al. 2013). The NPZ structure originated at a time when microbial plankton were typically considered as primarily phototrophic phytoplankton or heterotrophic protozooplankton. We now better appreciate that this represents a gross simplification; it transpires that much of the protist classically labelled as "phytoplankton" and as much as 50% of the "protozooplankton" in the photic zone are actually mixoplankton, combining photo(auto)trophy and phago(hetero)trophy in the same organism (Flynn et al. 2013, 2019). The "P" and "Z" in NPZ models are therefore behaving in a way that at least on occasion grossly misrepresents reality.

Mixoplankton express various forms of photo–phago mixotrophy; there is not one mixoplankton functional type (mPFT), but at the minimum two (Table 1). These two mPFTs are those that have a constitutive ability to photosynthese (CMs) and those that acquire that capability using photosystems taken from their prey or using symbionts (the non-constitutive mixoplankton, NCMs). The NCMs can be further divided into those that can acquire phototrophy from many phototrophic prey (generalist; GNCMs) and those that require specialist prey (SNCM) as plastidic forms (pSNCM)

Table 1   Definition of mixoplankton types, with examples of species

Mixoplankton type	Definition (after Flynn et al. 2019)	Examples
CM Constitutive mixoplankton	Protist plankton with an inherent capacity for phototrophy that can also exhibit phagotrophy (cf. NCM)	*Prymnesium* *Karlodinium*
NCM Non-constitutive mixoplankton	Protist plankton that acquires its capacity for phototrophy from prey or from endosymbionts (cf. CM)	see GNCM, SNCM
GNCM Generalist non-constitutive mixoplankton	NCMs that acquire their capacity for phototrophy from general (i.e. non-specific) phototrophic prey (cf. SNCM)	*Laboea* *Strombidium*
SNCM Specialist non-constitutive mixoplankton	NCMs that acquire their capacity for phototrophy from specific phototrophic prey (plastidic—pSNCM) or from endosymbionts (eSNCM)	*Mesodinium* *Dinophysis* Green *Noctiluca*

Definitions are after (Flynn et al. 2019). Examples for the mixoplankton types are given in Mitra et al. (2016) and Leles et al. (2017, 2019)

Table 2   Functionality of the protist model in each variant setting

Function	protoZ	GNCM	SNCM	CM	protP
Phagotrophy	●	●	●	●	○
Phototrophy	○	●	●	●	●
Acquired phototrophy		●	●		
Daily acquired phototrophy (poor management of acquisition)		●			
Interval acquired phototrophy (management of acquisition)			●		
Use of NH_4^+ with phototrophy		●	●	●	●
Use of NO_3^- with phototrophy		◑	●	●	●

The protist types are listed broadly in line with evolution. See also Table 1. Although nitrate usage is indicated as optional for GNCM (and was disabled in simulations shown here), it is also optional for the other phototrophic variants

Black circle = function expressed; white circle = function not expressed; black and white circle = function can be de/activated with a switch; no circle = function does not apply

protoZ protozooplankton, *GNCM* general non-constitutive mixoplankton, *SNCM* specialist non-constitutive mixoplankton, *CM* constitutive mixoplankton, *protP* phytoplankton

or with endosymbionts (eSNCM). This mPFT classification is described in full by (Mitra et al. 2016).

To date, there is only one model structure that attempts to simulate the variety of mixoplankton physiology (excluding eSNCM), namely the "perfect beast" model of Flynn and Mitra (2009) which provides a single variable stoichiometric (C:N:P:Chl) construct switchable between different modes of mixotrophy. Although the perfect beast model has been used in ERSEM-like simulators (Leles et al. 2018), the inherent complexity of a variable stoichiometric model can act as a hindrance to those who are hesitant to explore the implications of the inherently complex different mixoplankton strategies. This current work developed from a desire

to derive a construct that, while still describing the essence of the different mPFTs, is simple enough to operate within NPZ-style simulators.

The characteristics functions of the five protist variants portrayed in the model are shown in Table 2. These cover the range of functional types described in Mitra et al. (2016), with the exception of the endosymbiotic SNCM forms. The function types in Table 2 are arranged in the order in which phototrophy was added stepwise with increasing levels of integration of phototrophy with phagotrophy, beginning with purely phagotrophic protozooplankton (hereafter, protoZ), GNCM, SNCM, CM, and then finally (with the loss of an ability to perform phagocytosis) protist phytoplankton (hereafter protP). The protoZ align with "Z" in classic NPZ terminology and are incapable of phototrophy. The protP, "P" in classic NPZ terminology, are incapable of phagotrophy; the most ecologically important representatives of protP are the diatoms. We sought to build a model that could, by setting a few switch (parameter) values, enable a single construct to represent any one of these five protist forms. Within those forms, further modification can be made to fine-tune salient features affecting features such as prey selection, the relative roles of phototrophy and phagotrophy, the periodicity of ingestion of phototrophic prey for GNCM and SNCM, and so on.

These functional type descriptions hide a significant level of taxonomic variation. Thus, while many GNCMs are ciliates (Dolan and Pérez 2000; Pitta et al. 2001; McManus et al. 2004; Calbet et al. 2012; Mitra et al. 2016), the model would apply equally if one wished to consider flagellate GNCM. The SNCM is largely modelled in the image of the ciliate SNCM *Mesodinium* and the dinoflagellate SNCM *Dinophysis*. They are involved in the *Teleaulax–Mesodinium–Dinophysis* complex, where *Mesodinium* acquires its kleptochloroplasts from the cryptophyte *Teleaulax* (which itself may be a CM, feeding on bacteria) via ingestion and *Dinophysis* in turn acquires these chloroplasts from *Mesodinium* (Jacobson and Andersen 1994; Gustafson et al. 2000; Reguera et al. 2012; Yoo et al. 2017).

Methods

We provide a discursive description of the model here; the equations are provided in a linear form within an Excel file in the ESM to assist in deployment into the reader-preferred simulation software platforms. The model operates using ordinary differential equations. Figure 1 gives an overview of the submodels describing functionality in each of the five protist types, while Fig. 2 gives an overview of the entire NPZ-style model structure. In the ESM we provide additional information for the whole simulator as used here (i.e., including the abiotic submodel, and the

trophic connectivity). Nutrient N is provided as ammonium and nitrate, and light is provided in a light–dark cycle. References to additional figures in the Electronic Supplementary Material are identified in what follows in the style of "Fig. Sx". Some elements of the model exist for several organisms individually and are marked with a suffix indicating their affiliation (e.g. "_*Prot*"); suffixes are omitted here for clarity and simplicity.

Protist biomass is described as a single state variable for N-biomass ($mgN\ m^{-3}$); additional state variables are required when (as here) the model is run within a light–dark cycle, as intermediaries are required for calculating day average growth and photosynthetic rates. Depending on the value

Fig. 1 Schematic representations of the five protist functional type configurations. They contain the submodels for various physiological functions as indicated. *protoZ* protozooplankton, *GNCM* generalist non-constitutive mixoplankton, *SNCM* specialist non-constitutive mixoplankton, *CM* constitutive mixoplankton, *protP* protist phytoplankton. See also Tables 1 and 2. The microalgal prey, Alg1 and Alg2, have the same functions as protP
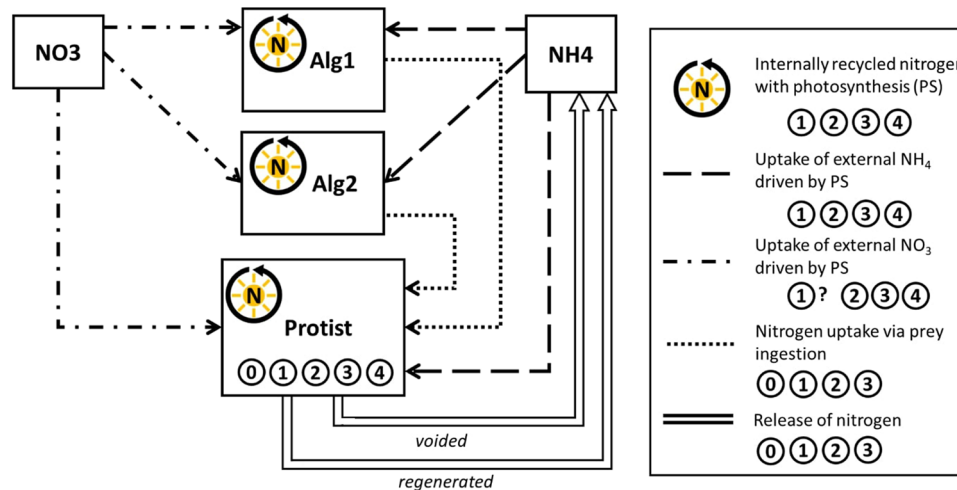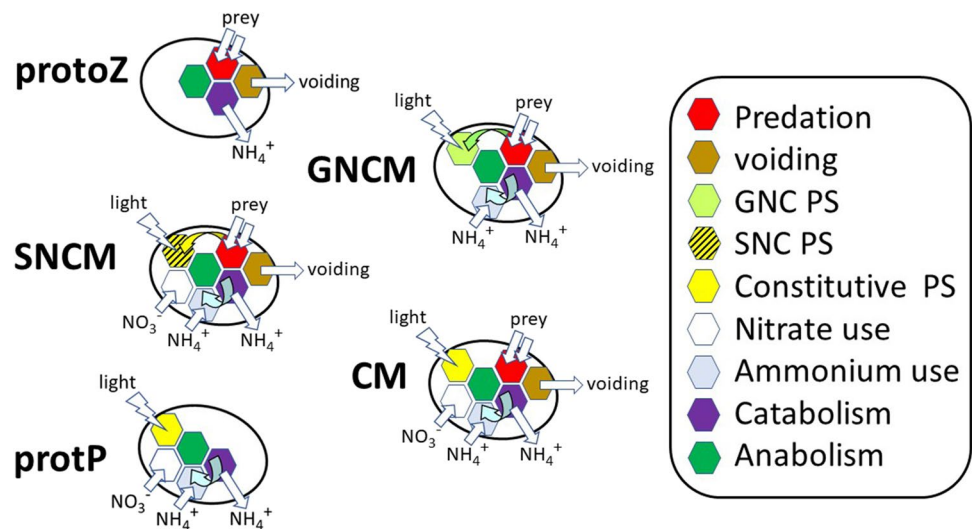
Fig. 2 Schematic of the main model and its state variables. The protist submodel can function as five different protist types (see Fig. 1, Table 2) by activating the respective physiology functions with a switch specific to the protist types. As an SNCM, the protist can prey on both Alg1 and Alg2 but only acquire chloroplasts from Alg1. The

priorities in the use of inorganic nitrogen types are: 1. internally recycled nitrogen, 2. NH_4^+, 3. NO_3^-. Effective use of external nitrate by GNCMs appears to be at best rare, which is why here this function was disabled (see also Table 2)

of a constant that acts as a switch (*Switch_Protist*; see ESM), the model conforms to the behaviour of one of five protist functional types. *Switch_Protist* takes the following values: 0 = protoZ, 1 = GNCM, 2 = SNCM, 3 = CM, 4 = protP. While the order of the protist functionality in evolutionary terms is likely akin to protoZ, GNCM, SNCM, CM and protP, for simplicity we will first describe protoZ, then protP, followed by CM, GNCM and SNCM.

There are also two prey types described in the model, termed "microalgae" (Alg1 and Alg2) which act as feed for protoZ, or as feed and/or competitors for mixoplankton and protP. The GNCM variant can acquire phototrophy by feeding on either of Alg1 or Alg2; the SNCM can also feed on both, but specifically needs to ingest Alg1 (as its specialist prey) to acquire its phototrophic potential. Functionally, Alg1 and Alg2 are analogous to the protP variant, and provide classic NPZ-style descriptions of organisms that could be considered as cyanobacteria or as protist "phytoplankton". The food web could be further developed as required, but an SNCM variant must make specific reference to one of the phototrophic preys (either to a CM, a protP or perhaps another SNCM, as appropriate to the purpose at hand) as the source of its acquired phototrophy.

protoZ variant

Only one state variable (N-biomass) is used with one inflow of nitrogen, in the form of ingested prey (*ing*). The approach used here to describe prey encounter, capture and ingestion is justified and described in detail by (Flynn and Mitra 2016) as modified in Flynn (2018). Encounter considers the allometric-based cell-specific encounter rate between predator and prey, where the cell numbers are calculated from carbon biomass and converted to N-biomass assuming fixed C:N stoichiometry. The encounter rate (*Enc*) per day is calculated after Rothschild and Osborn (1988) and makes reference to cell radius of protoZ and of prey (e.g., *r_Alg1*, ESD/2 in metre), prey cell number (*nos_Alg1*), speed of motilities (*v*) and water turbidity (*w*). Prey optimality for handling is considered by reference to the size of both predator and prey. A prey handling index (*PR*) defines whether prey size is in the suitable range for capture, indicating the likelihood of the predator successfully capturing it. In addition to prey handling and prey encounter rate, prey capture (*CR*) is also dependent on the palatability of the prey and the proportion of prey of optimal characteristics captured by a starved protist (*Optimal_CR*). The model contains a routine to reference palatability according to its N:C ratio and its toxicity (*tox*), though this is not implemented for this present work. The resultant capture rate is then multiplied by the prey:predator cell abundance ratio in *CRC*. If the prey biomass is above a certain threshold, actual ingestion (*ingC*) of captured cells is controlled by the maximum carbon-specific ingestion rate

(*ingCmax*; see below) and a constant for satiation control of ingestion (*KI*). If more than one prey type is available, *ingC* makes reference to the sum of captured cell biomass (*SCRC*); the ingestion rates are applied individually as outflows of the prey models (*lig*). To correspond with the otherwise nitrogen-based model, *ingC* is converted to nitrogen by reference to the N:C ratio (*NC_plank*).

The ingestion rate depends on its maximum possible assimilation of ingested material (*opmaxIAss*), which in turn depends on its demand for nitrogen to achieve maximum growth rate (*Umax*) accounting for losses and basal respiration (*BR*). The two outflows (Figs. 1, 2) are the release of regenerated nitrogen (*reg*) from catabolism and voided non-assimilated ingested material (*void*). The maximum possible ingestion rate (*opmaxIng*) satisfying *opmaxIAss* takes into account losses due to assimilation efficiency (*AEN*) and the specific dynamic action (*SDA*, anabolic cost for assimilating nitrogen). Ingested nitrogen lost by *SDA* is released as regenerated nitrogen (*regNsda*), while the non-assimilated nitrogen is voided (*voidN*). The growth rate (*u*) of the protoZ is the ingestion rate minus the rate of voiding and release of regenerated nitrogen. When *u* falls below a certain limit, biomass is further lost through a mortality rate (*mortRate*, Supplemental Material Fig. S1). Mortality increases gradually at *u* < 0 and attains a maximum value when *u* < negative half the *BR* rate assuming that below this threshold most of the population will die. The rate of prey ingestion depends on satiation (*opmaxIng*), prey optimality (*PR*), the encounter rate (*Enc*) of suitable prey and its capture (*CRC*); see Supplemental Material Fig. S7.

protP, Alg1 and Alg2 variants

These model variants are structurally the same as each other. Ammonium and nitrate assimilations are handled using a priority approach favouring ammonium, while photosynthesis uses a depth-integrated routine where the maximum rate is controlled by the N-status. (This routine can be replaced using one that makes reference to just the average at-depth irradiance level.) Only one state variable (N-biomass) is used. The phototrophic configuration of the protP and of Alg1 and Alg2 is described here identically with just minor differences in the photosynthesis parameterisation (slope alpha and the plateau maximum) to help differentiate them in model outputs. They could, of course, be made more or less different as required. For brevity, the following only makes reference to protP, but also applies to Alg1 and Alg2.

Dissolved inorganic nitrogen (DIN) uptake is needed to support the photosynthetic growth rate up to a maximum (*maxGPS*). DIN is acquired as nitrate and/or ammonium coupled to photosynthesis. In conditions where photosynthesis is less than respiration, ammonium is regenerated (*RegN*). DIN (as ammonium and nitrate) is taken up

according to Michaelis–Menten kinetics with a maximum value set by *maxGPS*, a half saturation constant for the substrate (*Knh4, Kno3*) and a scalar to define the transport needed to match to growth needs (*TGnh4, TGno3*). Through reference to the external DIN concentration, potential transport rates for ammonium (*PVnh4*) and nitrate (*PVno3*) are computed. The nutrient status (*Nu*) is contributed to by internally recycled (regenerated) ammonium (*RegN*), externally provided ammonium and externally provided nitrate, in that order of priority. The value of *Nu* down-regulates the achievable gross photosynthetic rate (*grossPS*) as described below. The actual nitrogen demand to support concurrent photosynthesis (*Ndem*) is corrected for the costs of assimilating DIN (metabolic respiration, *MR*). The difference of *Ndem* and *RegN* needs to be taken up as DIN (*uTP*). Organisms that can use both ammonium and nitrate prioritise ammonium; they take up nitrate (*Vno3*) if their nitrogen demand is not covered by the uptake of ammonium (*Vnh4*) and internal regenerated nitrogen (*RegN*).

Light and nutrient status (via *Nu*) limit photosynthesis. Photosynthetic efficiency (alpha, as the slope of the PE curve, *alphau*) depends on both quality of chlorophyll (*opAlphaChl*) and the (fixed) chlorophyll-to-carbon ratio of the organism (*opChlC*). Light is described as the photon flux density (PFD, µmol photon m^{-2} s^{-1}) and, in the implementation presented, is set within a light–dark cycle. Photosynthesis is described according to a depth-integrated variant of the Smith equation (Smith 1936; see Kenny and Flynn 2016), which takes into account light attenuation in the water column. Both water and suspended particles attenuate light; the growing biomass thus attenuates light and causes self-shading. Attenuation by chlorophyll [*abco_Chl*; 0.02 m^2(mg Chl)$^{-1}$] is used together with assumed fixed Chl:C and N:C stoichiometries values for each photosynthetic organism to derive the organism-specific attenuation coefficient (*abco*). Attenuation by this component then references the biomass abundance (mgN m^{-3}) to give *attco*. The total light attenuation in the water column is the sum of the light attenuation by all photosynthetic organisms and the water (*attco_W*) multiplied by the mixed layer depth (*MLD*; m). The negative exponent of the light attenuation (*exatt*; *EXP(-att_tot)*) is used in the calculation of the depth-integrated photosynthetic rate. The maximum photosynthetic rate under nutrient stress (*PSqmax*) the organism will achieve under optimal light conditions (*pytq*) depends on its photosynthetic efficiency described by the hyperbolic PE curve where *PSqmax* is the saturation factor. *Light* is the photon flux density expressed in units per day. The gross photosynthetic rate of the population in the water column (*grossPS*) is determined by integrating *pytq* over depth as a proportion of the light actually available after attenuation by water and photosynthetic organisms (*att_tot*). In darkness, the growth rate is decreased to zero; no mortality rate is implemented here

as within a reasonable time frame (weeks), phytoplankton typically survive in darkness consuming previously accumulated organic C (not explicitly simulated here in this N-based model).

See the end of the description for SNCM (below) concerning the enabling of the use of nitrate by protP.

CM variant

This variant merges the functionality of the protoZ and protP variants (see above and Fig. 1), placing an obligatory requirement for a stated level of phototrophy while permitting enhanced growth when operating as a mixoplankton. Only one state variable (N-biomass) is used. Constitutive mixoplankton have an inherent capability for photosynthesis. In addition, they can acquire organic nitrogen through prey ingestion. Like the protP, the CM does not have a mortality rate when the growth rate becomes very small.

Growth is controlled differently from the protP and protoZ variants, because phototrophy and phagotrophy are coupled. The configuration of the CM prioritises phototrophy, with any difference between the maximum growth rate and net phototrophy (*PAss*) being topped up via phagotrophy. While growth as a mixoplankton can exceed that of growing solely as a phototroph, there is the operational caveat that a critical amount of nutrient must come via phototrophy. This minimum proportion of the maximum growth rate to come from phototrophy is set by *pCritMin*; it accounts for the need to obtain certain metabolites via photosynthesis. The maximum assimilation of ingested material (*maxIAss*) can therefore not be higher than *maxGU,* defined as gross assimilation needed to support *Umax,* minus the critical amount of phototrophy (*op_pCritMin*). The operational maximum assimilation of ingested material (*opmaxIAss*) cannot exceed *maxIAss* or fall below *BR* (e.g., in darkness); the latter permits survival but not positive growth when feeding in darkness, unless *pCritMin* = 0.

See the end of the description for SNCM (below) concerning the enabling of the use of nitrate by CM.

GNCM variant

This variant merges the functionality of the protoZ and protP variants (see above and Fig. 1), but here without an ability to use nitrate and also a need for phagotrophy of photosynthetic prey to provide phototrophic potential. Like the CM variant, there is an obligatory requirement for a stated level of phototrophy. NCMs do not have an inherent capability for phototrophy and thus need to acquire their phototrophic ability (chloroplasts) from their phototrophic prey. Ingestion and phototrophy are therefore much more closely linked than they are in the CM variant. In addition to the single state variable describing N-biomass, the GNCM variant makes

use of an additional state variable to track the history of the acquired phototrophic potential, which decays over time in the absence of recent photosystem acquisition. The maximum photosynthetic growth rate is maintained as long as the GNCM ingests at least a minimum number of chloroplast-containing prey items per day and decreases at lower ingestion rates. The ingestion rate of chloroplast-containing prey, relative to the minimum required to support maximum phototrophy is indexed by the prey ingestion index (*PiI*). *Strombidium capitatum* reportedly replaces its chloroplasts after 40 h (Schoener and McManus 2012). Such minimum requirements are computed through reference to prey:GNCM cell ingestion rates. Noting that GNCMs simply asset strip their prey's photosynthetic machinery, the maximum photosynthetic growth rate of the GNCM is a combination of the maximum photosynthetic growth rates of their ingested prey species in proportion to the ratio they were ingested in. As GNCMs have very limited control over the performance of their chloroplasts, the same applies to the photosynthetic efficiency of the chlorophyll (*alphaChl*) and the chlorophyll carbon ratio (*ChlC*). We note that increasing gross growth efficiency is dependent upon the carbon from photosynthesis being sufficient to re-assimilate SDA-released ammonium (Schoener and McManus 2017). If the rate of fixed carbon is low relative to the rate of ingestion, then this may result in an inability to recover the ammonium; it may just balance *BR*, for example. However, under a high-prey scenario, the need to retain nutrients is lessened.

See the end of the description for SNCM (below) concerning the enabling of the use of nitrate by GNCM.

SNCM variant

This model variant merges the functionality of the protoZ and protP variants (see above and Fig. 1), placing an obligatory requirement for a stated level of phototrophy and also for phagotrophy from a specific prey source to provide phototrophic potential. This variant (like the GNCM variant) makes use of an additional state variable to track the history of the acquired phototrophic potential. The SNCM differs from the GNCM in its ability to control the ingested chloroplasts and that it can only use the chloroplasts of one prey species (set here as *Alg1*). SNCMs are known to be able to maintain maximum photosynthesis with their acquired chloroplasts up to 30 days or longer. The prey ingestion index (*PiI*) of the SNCM records the ingestion rate of the special prey over the last 30 days (or any other critical time frame) (Park et al. 2008; Hansen et al. 2016). *Mesodinium* reportedly can survive up to 100 days without prey (Johnson et al. 2007; Hansen et al. 2016) and *Dinophysis* up to 30 days (Hansen et al. 2016), with *D. caudata* surviving for up to 2 months (Park et al. 2008). In the absence of continuing chloroplast acquisition from the special prey, the operational

maximum photosynthetic rate gradually declines, described here using a hyperbolic function.

Due to its ability to control the performance of the chloroplasts, the SNCMs *opPSmax*, *alphaChl* and *ChlC* are all inherent to the mixoplankton protist and not to its prey, as is the case for GNCMs. However, these photosynthesis parameters are modulated by the prey ingestion index (*PiI*), applied now specifically with reference to the special prey (here, Alg1). For both the GNCM and the SNCM, the degree of similarity in the functioning of the chloroplast in the prey and the host can be changed by making alpha either dependent or independent of the host.

The ability to use nitrate can be switched on or off for all mixoplankton types and also in the protP, as required to conform to the physiology of the organisms of interest. Thus, while GNCMs are typically suspected to lack an ability to use nitrate, *Strombidium rassoulzadegani* (Schoener and McManus 2017), can use nitrate (Schoener and McManus 2012). In the SNCM *Mesodinium*, the ability to used nitrate appears to be linked to chloroplast possession (Wilkerson and Grunseich 1990). This switching is achieved by changing value of *TGno3_Prot* from 1.1 for nitrate use to 0 to turn nitrate use off.

Simulations

The model was built and run using Powersim Studio 10 (www.Powersim.com); the Studio 10 model is provided in the ESM. For the simulations presented here, the model was run using an Euler routine to solve ordinary differential equations, with a step size of 0.0625 day^{-1}. For illustration, growth of the protist (configured as one of the 5 variants) is simulated over a 30-day period also with microalgae Alg1 and Alg2. Steady-state and dynamic sensitivity analyses were conducted, the latter using the "risk" tool in Studio 10, using a Latin hypercube sampling routine.

Results

Sensitivity analyses

To test the model's sensitivity to the value of constants controlling protist behaviour, functional dependence and dynamic state sensitivity analyses were performed. The numeric results of both analyses can be found in the ESM. The most sensitive parameters for the protist model alone are assimilation efficiency (*AEN*), *BR* rates, the maximum proportion of growth that can come from phototrophy (*pCritMax*), and the maximum growth rate (*Umax*). In the dynamic sensitivity analysis, performance of the whole model showed sensitivity to the same parameters, and additionally also to the anabolic respiration cost for assimilating DIN (*MR*).

For operation as a GNCM or SNCM, the critical minimum ingestion index (which affects the dynamics of the acquisition of phototrophy) showed sensitivity. None of these levels of sensitivity were considered as being excessive in terms of the effect changing of the value of the constant would have on the general production of the organism. All are in the direction and of the magnitude expected. A lowering of the assimilation rate for example drives up the ingestion rate pro rata, as expected.

Functional dependence

Figure 3 shows, for each of the protist functional types, the net growth rate at different combinations of light and prey abundance. The protoZ and protP plots provide references against which to judge the performance of the mixoplankton. Note that in all instances the maximum growth rate was set at the same value, and indeed as far as applicable (see Table 2) all constants were of the same value. It is evident that all mixoplankton configurations have emergent features of lower half saturation points for light and prey abundance than do the protP and protoZ variants. The protP does not attain growth rates near the maximum (0.693 day^{-1}) until PFD > 500 µmol photons m^{-2} s^{-1} (not shown). The mixoplankton do much better in this regard even at low prey abundances, because they acquire additional nutrition via predation. The form of the GNCM vs SNCM plots reflect the fact that the former cannot (as configured here) use nitrate and thus grows phototrophically using ammonium regenerated by prey digestion; no external ammonium was supplied for these particular model solutions. It is also noteworthy that there is no net growth for GNCM or SNCM with zero prey; these protist configurations acquire their phototrophic potential from ingestion of their phototrophic prey.

Figure 4 shows how the differences in behaviour in Fig. 3 have potential to define niches for the different protist configurations versus protoZ. The protoZ is only superior against GNCM at very low light, and GNCM is superior mainly at low prey abundance (noting a critical prey availability is required to support acquired phototrophy); otherwise they are quite similar. A similar trend is seen for SNCM v protoZ, except SNCM is superior to GNCM at low prey, because SNCM can use nitrate while GNCM here relies solely on recovery of ammonium from prey digestion to support phototrophy. This also explains the difference between SNCM v GNCM. CM is superior to protoZ at even low prey availability, and is likewise superior to GNCM and SNCM, because CM does not depend on ingestion of phototrophic prey for acquired phototrophy.

Figure 5 is analogous to Fig. 4 but now defining niches for the different protist configurations versus protP. Superiority of protP over protoZ relies on the absence of prey and the presence of sufficient light (nitrate nutrient being supplied

in abundance in these simulations). In comparison, GNCM is equal to protP at zero light as GNCM is critically dependant on a minimum level of phototrophy and so cannot grow solely phagotrophically. Similarly, SNCM and also CM are also reliant on low light to grow even with abundant prey. At very low prey levels, GNCM and SNCM are disadvantaged in comparison with protP by the need to acquire phototrophy from their prey. However, CM is superior to protP over the entire prey–light range, although it too cannot achieve net positive growth in total darkness, hence the difference between protoZ and CM at 0 PFD (i.e., darkness; Fig. 3).

Dynamic simulations

Figure 6 shows how each of the protist descriptions behave in dynamic scenarios under different light and nutrient regimes. The system is conservative, with system nitrogen (*sysN*) as the sum of dissolved nitrogen and biomass-N being constant. Details for different facets of these interactions are shown in Figs. 7, 8 and 9, and Supplemental Material Figs. S4–S8. Light is affected by the *MLD* and also by the self-shading that develops as the supplied inorganic N is converted to Chl-containing biomass (Supplemental Material Fig. S5). As the inoculation (initial biomass value) of the protist is half that of either of the algae, the increase in algal (Alg1 and Alg2) biomass is more obvious at the start of the simulations. Growth of the protist follows that of Alg1 and Alg2 with a delay that is greater according to the level of heterotrophy (i.e., the matching of protist growth with that of Alg1 and Alg2 was closest in the order protP ≥ CM > SNCM > GNCM > protoZ). This reflects the need of protists dependent on phago-heterotrophy for sufficient prey abundance to support their growth; the more dependent the protist type is on the ingestion of prey to grow, the more it requires the prey biomass to increase first to effectively support its own growth. Below, we first consider the configuration-specific results from these dynamic scenarios, and then we consider more general results.

protoZ

When the protist is set as protoZ, the model behaves like a typical NPZ model. Ammonium and nitrate (in that order of selection) decrease as they are consumed by Alg1 and Alg2 (Fig. 6). The increase in algae biomass is followed by a rapid rise in the protoZ biomass. Following the voiding of non-assimilated biomass (with its assumed instantaneous remineralisation in this model) and release of regenerated nitrogen by the protoZ, ammonium levels increase while the algal biomass is removed by predation. On near extinction of the algal prey, protoZ starve and die, further contributing to the ammonium concentration. Ammonium reaches a maximum on the effectual death of all protoZ. The
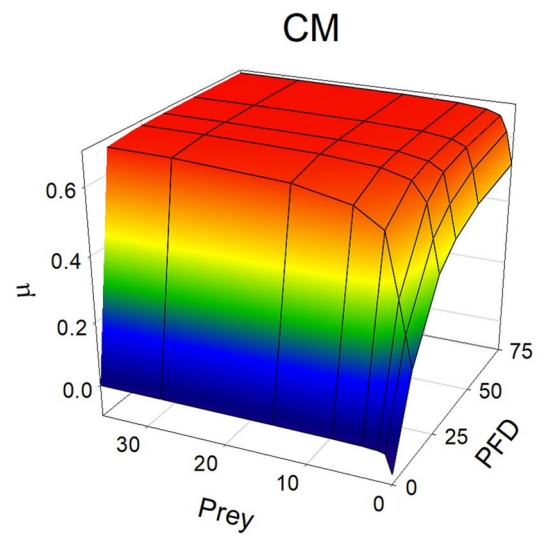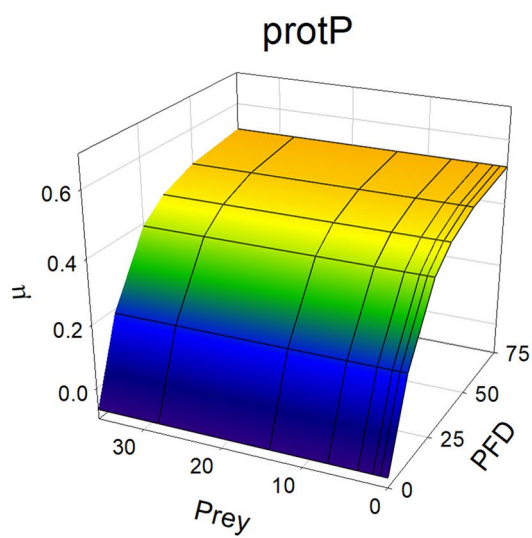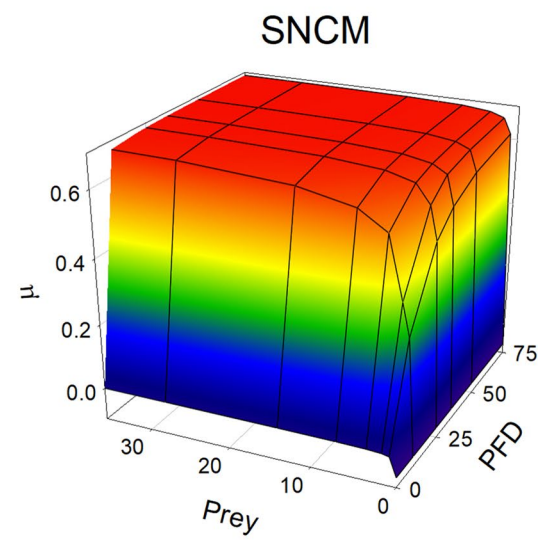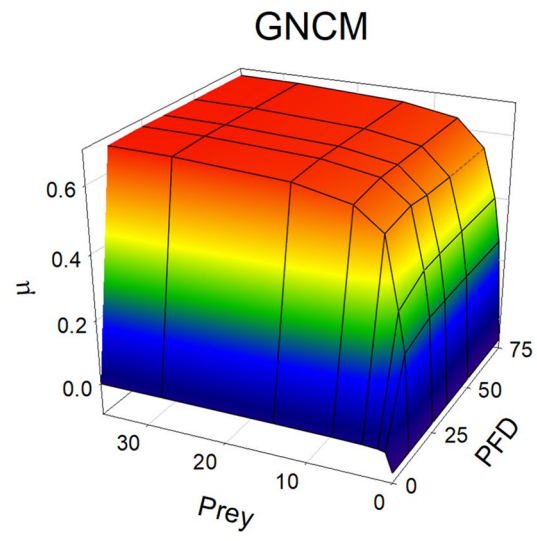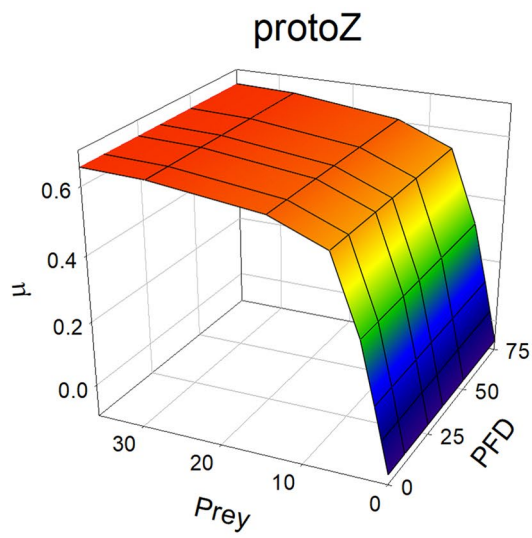
◄**Fig. 3** 3D-mesh pots showing the relationship between growth rate (μ; day^{-1}) and sources of energy supplied as light (PFD; μmol m^{-2} s^{-1}) or prey (mgN m^{-3}) for different protist configurations. Nitrate is supplied as the sole external N source, at 700 mgN m^{-3} (50 μM) Prey are phototrophic and assumed also to be the special prey species required to support acquired phototrophy by the SNCM. Protozooplankton (protoZ) and protist phytoplankton (protP) can only use prey or light, respectively. GNCM as configured here cannot use nitrate and hence are solely reliant upon inorganic N regenerated from digestion of prey. SNCM can use nitrate, explaining the differences between SNCM and GNCM configurations. However, both GNCM and SNCM must also engage in predation to acquire phototrophy. CM can engage in phototrophy in the absence of prey. Note that the relationships for growth vs PFD and prey for GNCM, SNCM and CM are all steeper than for their protoZ and protP comparators

pattern of rapid increase and decline in biomass is mirrored by the growth rate of the protoZ (Fig. 7); after a peak, the growth rate rapidly declines and becomes negative as prey consumption fails to meet respiratory demand. The predator–prey cycle is more frequently repeated in low nutrient ("oligotrophic") conditions (Fig. 6), as the interactions are less affected by boom-and-bust dynamics when both algal and predator growth are restrained by resource abundance. At around day 15, the protoZ's growth rate increases again at a slower rate than previously, but reaches a higher value and a plateau before it collapses again. At greater *MLDs*, the dynamics were slowed with decreased prey growth rates at lower light levels, contributed to also by self-shading from high algal biomass. Algal growth rates increase again when light limitation (self-shading) is relieved by predation decreasing the total algal biomass. In conditions with lower nutrient loads, events are prolonged as prey availability limits the predator. At high nutrient loads, growth of the algae is prolonged due to biomass-linked self-shading causing light limitation (Supplemental Material Fig. S5).

GNCM

Despite their shared high level of dependency on phagotrophy, the simulations using the GNCM display certain differences to those using the protoZ. For one thing, growth commences earlier for the GNCM (Fig. 6). This is due to two factors: (1) once the GNCM becomes phototrophically active from consuming Alg1 and/or Alg2 it increases its growth rate, (2) as the ammonium released with *SDA* is recovered (rather than being released, as in protoZ), the conversion of prey capture to protist growth is greater than it would be for a protoZ for a given grazing rate. The GNCM grows by coupled photo–phago-trophy thus becoming also a competitor for ammonium and light to the algae. The GNCM growth rate exceeds that of the algae, because the protist is not so limited by light attenuation and can in addition feed on the algae. Rather than displaying a short-duration biomass peak, the growth rate of the GNCM remains higher for

longer—the duration of the plateau in growth rate is affected by MLD and nutrient load (Fig. 9)—before the steep decline. Ammonium did not accumulate as it did with the protoZ version, and nitrate usage by the algal prey (GNCM not being allowed to use nitrate in these simulations) became more apparent. Since the GNCM prioritises phototrophy as long as the conditions for it are opportune (Fig. 7, low nutrient load/self-shading and *MLD*), they exert a lower grazing pressure on the algae than do protoZ, thus allowing the algae to achieve a larger biomass than in the protoZ scenario. The GNCM also generated larger peak biomasses than the protoZ, particularly in shallower *MLDs*. Once the algae prey are consumed, the GNCM growth rate falls, as it can no longer perform acquired phototrophy. Like the protoZ, the GNCM then immediately begin to starve and die. When the protist operates as a GNCM, any second bloom cycles starts with a much greater delay than when operating as a protoZ, because the GNCM grazes down the prey more completely.

SNCM

The SNCM grew for longer and generated much more biomass during blooms than the GNCM variant. In addition, nitrate levels declined further and faster than when the protist was a GNCM, because the SNCM is also able to use nitrate in addition nitrate usage by the Alg1 and Alg2. The net phototrophic growth rate is also more stable as the SNCM can use nitrate in addition to ammonium. On exhaustion of resources, the growth rate of the SNCM declines at a much slower rate than does the GNCM variant, as it has a much less frequent demand of prey ingestion than does the GNCM. Just as the GNCM outperformed the protoZ in biomass yield in shallow and oligotrophic conditions, so the SNCM outperformed the GNCM in those conditions. The explanations are that: (1) the SNCM needs to ingest prey much less frequently than does GNCM to maintain its acquired phototrophy capability, making it more independent of the biomass of its prey and (2) it can use nitrate granting it an additional source of nitrogen especially in oligotrophic conditions.

The ability to photosynthesize and thence use inorganic nitrogen only gives the NCMs an edge over protoZ under good light conditions (Fig. 4). In deep highly eutrophic water, light attenuation is so high (Supplemental Material Fig. S6) that they have to resort almost completely to phagotrophy (noting that a critical proportion of N must nonetheless come via phototrophy). This also affects the use of ammonium vs nitrate. In the SNCM configuration, the ratio between nitrate and ammonium usage reverses (*f*-ratio goes low, Supplemental Material Fig. S8) at the end of the bloom with ammonium exceeding nitrate usage in oligotrophic conditions until 40 m and mesotrophic conditions until 10 m. As long as the SNCM can acquire sufficient photosynthetic
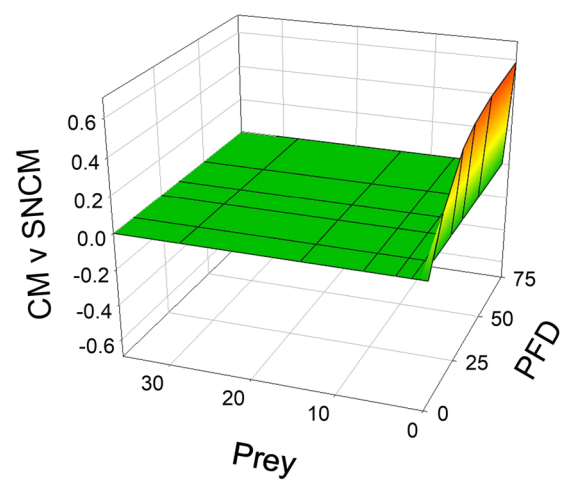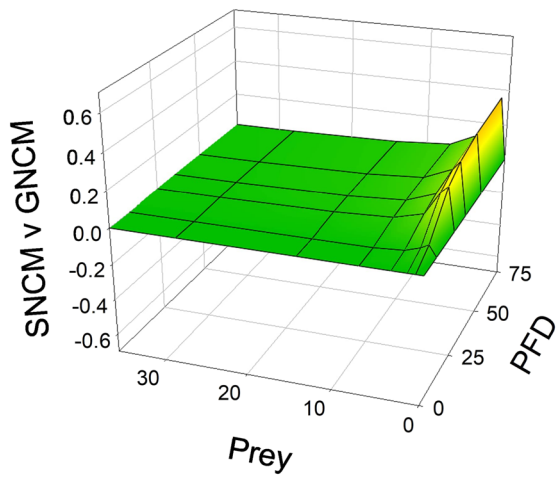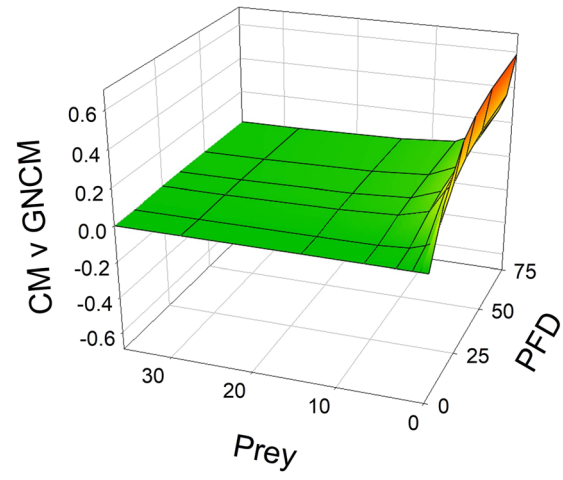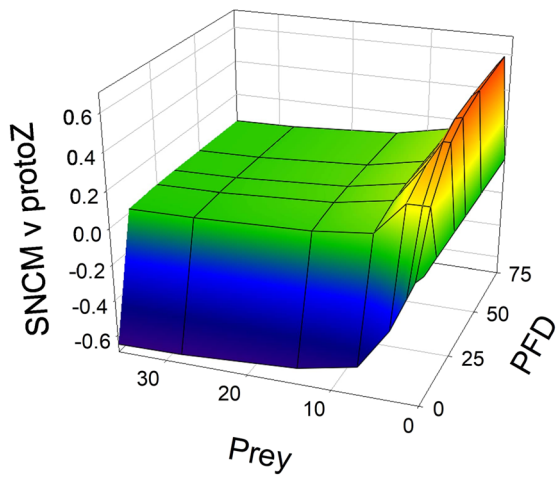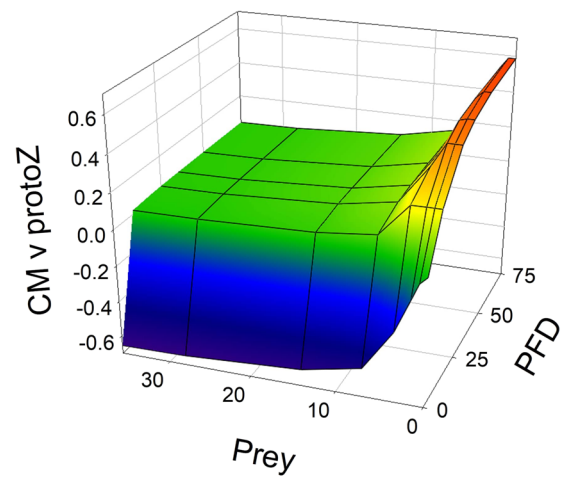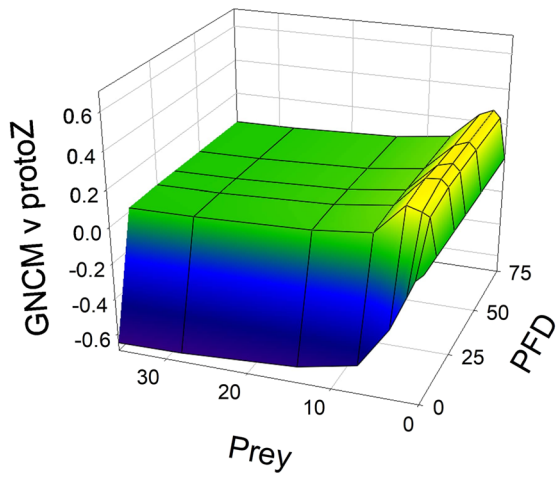
◀**Fig. 4** 3D-mesh plots providing niche comparisons between pairs of protist variants excluding protP (see Fig. 5). These are based on the relationship plots shown in Fig. 3 between growth rate and sources of energy supplied as light (PFD; μmol m^{-2} s^{-1}) or prey (mgN m^{-3}). The z-axis shows the difference between the growth rate (μ; day^{-1}) of the first named protist type and the second named; a positive value indicates a niche where the first named is superior, a negative where the second named is superior

capacity from their prey, they can also use nitrate, as their internally recycled ammonium is insufficient to meet their needs in primary production. Indeed, they can become net contributors to DIN and ammonium starts to accumulate.

CM

The CM configuration differs from the NCMs in that the former can commence growth without needing to acquire phototrophy from ingesting phototrophic prey. In addition, after depletion of prey, the CM can continue growing by phototrophy alone. The CM thus remains as an established bloom, because it does not have the starvation-associated death rate seen in the other phagotrophic forms. This configuration attained the maximum possible biomass, all as just CM (the algae having been eliminated), under any nutrient load and *MLD* (taking longer to do so with lower light attributed to a deeper *MLD* and/or self-shading at high nutrient loads). It not only competes with the algae for nutrients (actually outcompeting them, because phagotrophy contributes to CM biomass growth), but also removes its competitors for light by feeding on them in light-limiting conditions. The CM growth rate is similar to the SNCMs, but develops more smoothly and does not eventually go negative.

protP

The protP growth dynamics are the same as the two algal organisms as it functions identically (noting that its Chl:C is configured as being like Alg1, while Chl:C for Alg2 is lower). The growth rate of the protP is equal to the net phototrophic growth rate of the CM after the latter runs out of prey. Here, the algae accumulate biomass faster than they do in the presence of a phagotroph (protoZ or mixoplankton), because of the lack of grazing pressure. By the same token, growth of protP biomass is slightly slower than the mixoplankton, because it does not have the added advantage of phagotrophy and is restricted by light availability in dense blooms. The protP biomass does not surpass that of either of the algae, which is a consequence of the lower inoculum (start biomass value) of the protist. Like the CM, protP continues to grow until nitrate is depleted, and then remains at that established high biomass. The overall biomass yield of all organisms in the protP scenario (i.e., Alg1 + Alg2 + protP) equals that of the CM alone in the

CM variant simulations. The CM removes its competition and then uses all nutrients in the system for itself, whereas when the protist is configured as protP the three organisms (Alg1 + Alg2 + protP) have to share the DIN.

General results

Under any given combination of nutrient loading and *MLD*, the functional configuration of the protist greatly influences the use of external nitrogen and the development of the biomass of the different components algal and protist biomass (Fig. 6), and thence affects cumulative productivity (Supplemental Material Fig. S4). Not only are there clear differences between the simulations using a protP vs mixoplankton, and mixoplankton vs protoZ, but there are clear differences between the different mixoplankton types (i.e., GNCM vs SNCM vs CM). Increased nutrient loads generally lead to larger yields in the biomass for both the algal prey/competitors and protist. Configuring the protist as a protoZ generated the lowest total biomass, as this form cannot contribute directly to primary production. The protist peak biomasses were highest in the mixoplankton settings, with the SNCM and CM configurations both surpassing the GNCM version. Configured as a mixoplankton, the protist outcompeted its algal prey in all three modes (GNCM, SNCM, CM). As protP, the protist was an equal competitor to the algae resulting in the final overall biomass level of the three phototrophs combined being similar to that of the CM alone. Under all protist configurations, additional bloom cycles are seen if the simulation is played out over longer periods (not shown). The gap between cycles increased with nutrient load and degree of phototrophy in the protist; the SNCM simulation failed to repeat a cycle even after 500 days due to a failure of its Alg1 photosystem donor to regrow.

The maximum instantaneous prey assimilation rate is a constant in the protoZ configuration, and there is no diel oscillation. In contrast, the mixoplankton configurations have a variable operational maximum prey assimilation rate that depends on the concurrent photosynthetic rate, and therefore varies between a maximum value and that required to just match *BR*, and also with the cycle of illumination. As the mixoplankton can only (re)assimilate the ammonium released by *SDA* during assimilation of prey N concurrently with photosynthesis, their prey ingestion only takes place during the light phase. The changing maximum ingestion rates in the mixoplankton configurations result in their food lasting longer.

Physiological features

All phototrophic organisms in the model prioritise the use of ammonium (Fig. 8). Once, ammonium levels become insufficient to support growth, the algae, SNCM, CM and protP
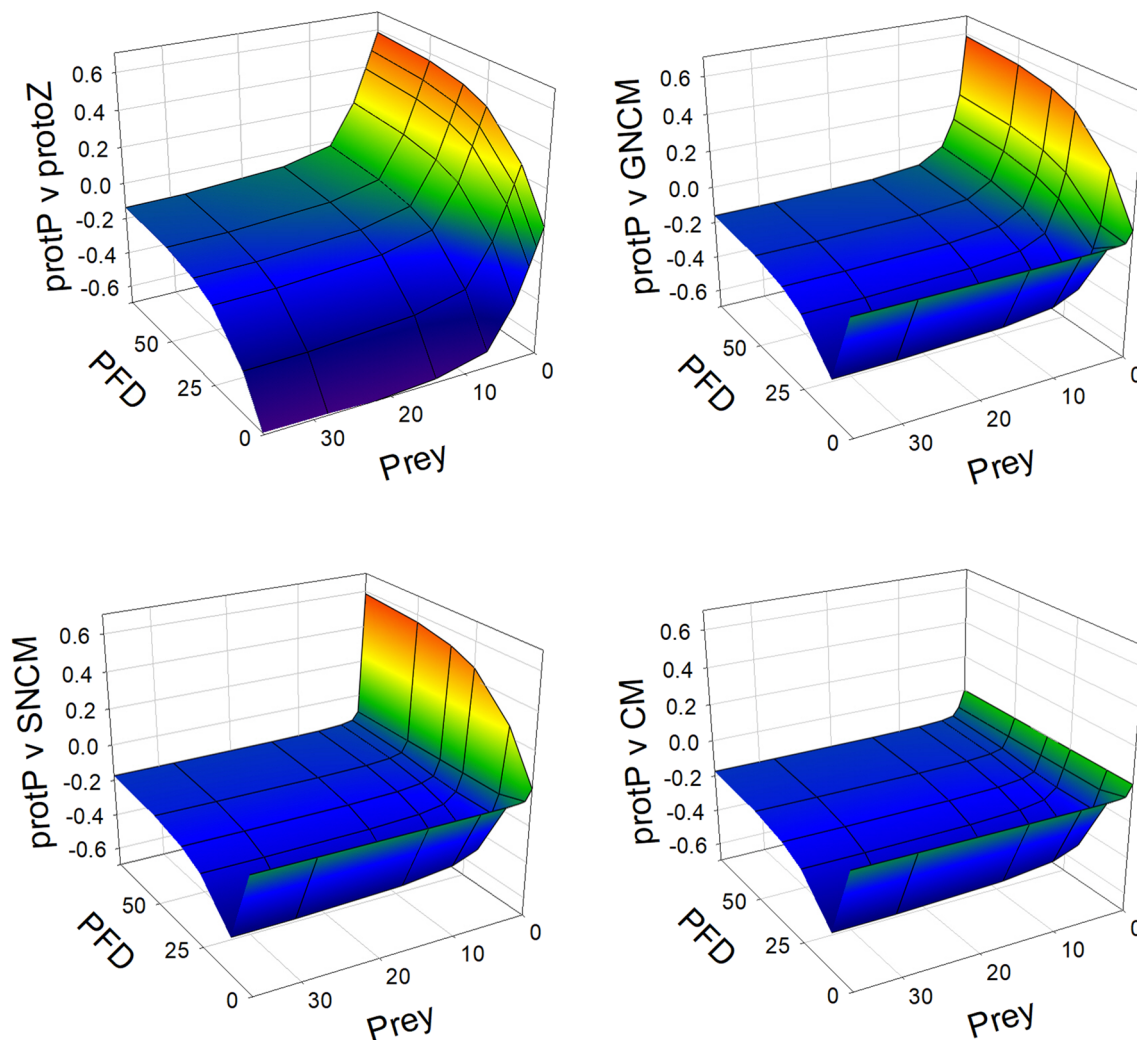
Fig. 5 As Fig. 4 but for niche comparisons between protP and the other protist configurations. Note that for clarity the rotation of the 3D mesh is different to that used in Fig. 4

begin to take up nitrate to achieve maximum growth rate. The NCMs only use inorganic nitrogen as long as prey are available, as they require those prey to provide their photosynthetic potential. The balance of nitrate and ammonium usage, and the specific rates of usage are affected by the degree of light limitation and the rate of ammonium regeneration (which, for mixoplankton, is affected also by internal ammonium recycling). The decrease in the use of ammonium does not stem from limitation in ammonium, but due to light limitation associated with high phototrophic biomass causing self-shading (Supplemental Material Fig. S5).

Under high nutrient load, with a high initial organism inoculum, the encounter rate of prey is greater. Phagotrophs feed at their maximum capacity, outstripping the environment of their prey faster, in conditions with high nutrient load. When prey concentrations fall below the minimum concentration, below the threshold to sustain the NCMs minimum chloroplast demand, NCM mixoplankton lose their phototrophic ability.

In Supplemental Material Fig. S5, the biomass levels of all five protist configurations are shown growing under combinations of nutrient loading and *MLD* that would yield similar depth-integrated levels of irradiance. Except for the development of biomass of the protoZ in oligotrophic conditions at 40 m, the levels of nitrate, ammonium, the two algae and the protist show similar patterns for a given protist configuration. Differences between simulation scenarios in Fig. 6 are thus most strongly driven by the impact of irradiance. Light limitation (Supplemental Material Fig. S6) affects energy inputs and thence the organism growth rates and system dynamics. The behaviour of the SNCM is like an intermediate between the very different GNCM and CM in this context.
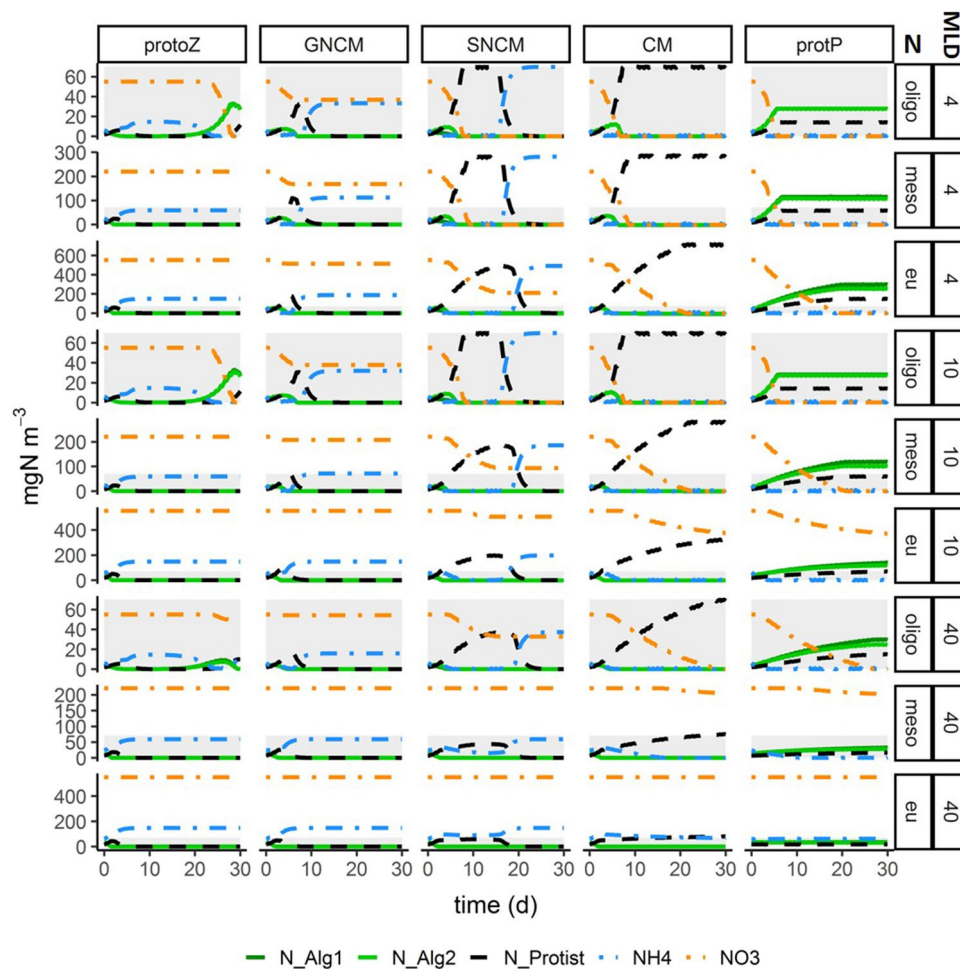
Fig. 6 Changes in biomass and nutrient concentrations in simulated systems of different nutrient loading (oligo-, meso- and eutrophic) and mixed layer depth (*MLD*; 4, 10 and 40 m). In all instances, two phototrophs (Alg1 and Alg2) are present as competitors and/or prey for the "Protist". Dissolved inorganic nitrogen (DIN) is present as nitrate (NO_3^-) and ammonium (NH_4^+). The "Protist" is configured, as indicated in columns left to right, as microzooplankton (protoZ, which can consume both Alg1 and/or Alg2), GNCM (which acquires phototrophy from consumption of Alg1 and/or Alg2), SNCM (which acquires phototrophy only from Alg1, but can graze on both Alg1 and Alg2), CM (which can consume both Alg1 and/or Alg2, but has its own phototrophic potential), and as a non-phagotrophic protist phytoplankton (protP). Alg1 and Alg2 were each inoculated at a N-biomass abundance equal to 5% of initial DIN, while the protist was inoculated at 2.5% of initial DIN. The chlorophyll–carbon ratio of Alg2 (*ChlC_Alg2*) was 0.05, while that for Alg1 was 0.06 so to create a slight physiological difference between the two prey species. The grey box indicates the maximum nutrient load in the oligotrophic scenario to facilitate comparison between the different nutrient loads

Discussion

Model overview

We describe a low computation cost protist model that can be readily configured to represent different protist plankton types, physiology, size and growth rates. The model explicitly considers allometry for prey encounter kinetics and also the acquisition of chloroplasts into NCMs. The model as presented allows for comparing performances of these protist types in different conditions of water depth, nutrient load and irradiance. Thus, the model provides a useful tool to explore hypotheses and questions concerning plankton

dynamics under different scenarios. As a nitrogen-based model with few state variables, it is simple and runs fast. It is therefore suitable for implementation in large ecosystem dynamic models that use plankton models.

The subject of plankton trait trade-off has provided a rich ground for theoretical research over the last few decades, including for mixoplankton (Thingstad et al. 1996; Stickney et al. 2000; Hammer and Pitchford 2005; Ward et al. 2011; Berge et al. 2017). Much of this literature not only makes assumptions of mixoplankton physiology that are not supported by rigorous analysis, but the models lack flexibility for configuring in line with different MFTs (Flynn et al. 2019). Mixotrophy is not simply an addition of phototrophy

Fig. 7 Daily averaged (of light and dark) growth specific growth rates. uTP values are day-averaged net photosynthesis (which for the Alg1 and Alg2, and also for protP, is the growth rate), while for the protoZ and mixotrophs, the day average is designated as *u*. For mixotrophs, *u* is the total growth rate of combined phototrophy and phagotrophy. The rows indicate *MLD* (4, 10 and 40 m) and nutrient load (oligo-, meso- and eutrophic, Electronic Supplementary Material Table S1)
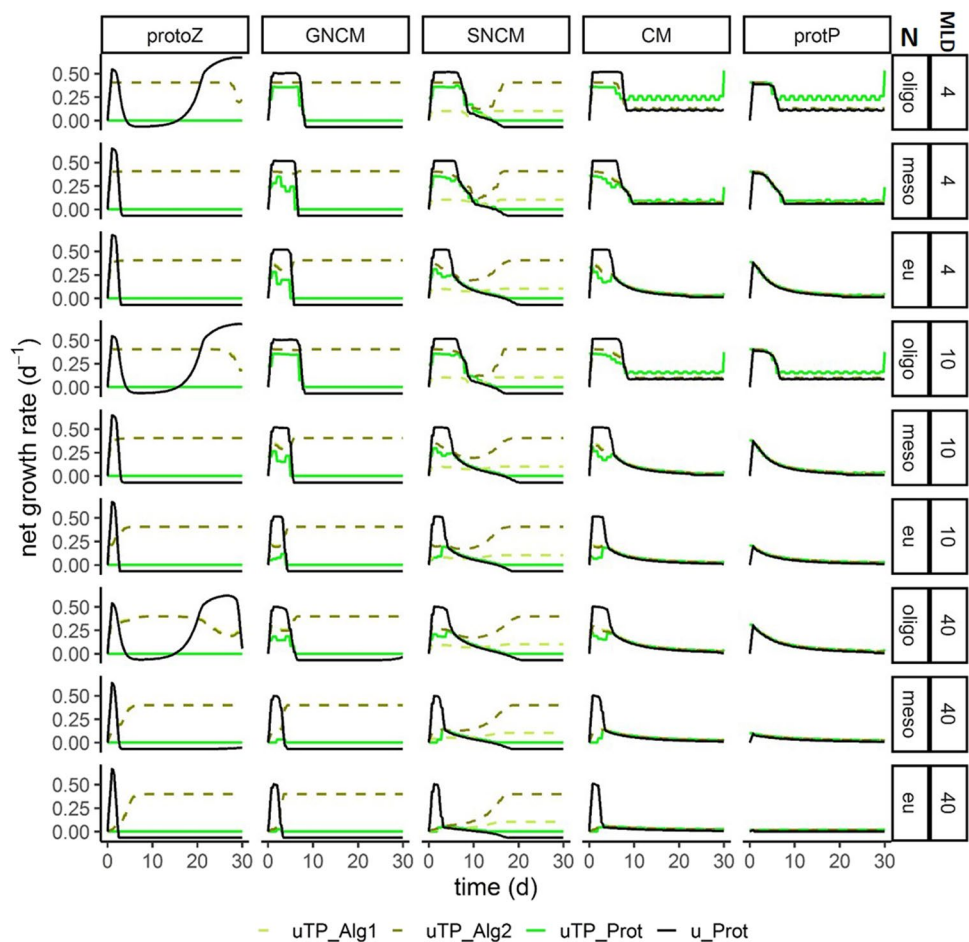

and phagotrophy, to be described in models by employing a common simple set of additive equations (Mitra and Flynn 2010), and neither is it so simulated here. There is a synergism that is important for mixoplankton physiology, and that differs radically between CM and NCM variants. While the CM variant prioritises phototrophy, provided that a certain proportion of nutrition comes via that route, it can be configured to grow faster under mixotrophy. The NCMs have an essential requirement for phagotrophy and also phototrophy, but again elevated growth rates require close coupling of phototrophy and phagotrophy. The competitive functioning of these mixoplankton can also not be judged readily by reference to resource acquisition. If we consider just the rate of phagotrophy, for example, then for a given growth rate a mixoplankton may indeed appear inferior to the protoZ in terms of ingestion; however, by virtue of recovering the *SDA*-attributed loss of ammonium (ca. 30% of assimilated N) the conversion efficiency is much higher. Similar arguments can be made for comparisons of phototrophy in protP versus that in mixoplankton. The consequences of mixotrophy can be seen from our simulations where, assuming all else is equal, the effective half saturation concentration of

nutrient or prey can be seen to be lower in comparison with non-mixotrophic competitors (Fig. 3).

Most models considering mixoplankton describe only one functional type (e.g., Faure et al. 2019). The simplicity of our model allows inclusion of a broader variety of mixoplankton functional types and thus an improved level of representation within a single simulation platform. The sensitivity analysis (Supplemental Material Fig. S2 and S3) indicates which parameters most influence growth and functioning of the organism and are thus factors upon which most emphasis should be placed in experiments. These include respiration and assimilation efficiency, as well as the expected sensitivity to the maximum growth rate. *AEN*, *BR* and costs of assimilating DIN (*MR*) all influence the efficiency with which the protist uses the acquired nitrogen. Thus, these parameters affect the proportion of nutrient and prey uptake to growth of the protist. The maximum proportion of growth supported by phototrophy alone (*pCritMax*) determines whether the protist is vulnerable to prey scarcity or the relative role of phototrophy. As this model assumes a fixed stoichiometry, it will not be as sensitive to parameters related to stoichiometry as a model with variable

Fig. 8 Daily averaged rates of
inorganic nitrogen uptake by
the phototrophic protist variants
in oligo-, meso- and eutrophic
conditions and in three different
mixed layer depths (*MLD*, m).
Vno3 and Vnh4 are the uptake
rates for nitrate and ammonium,
respectively
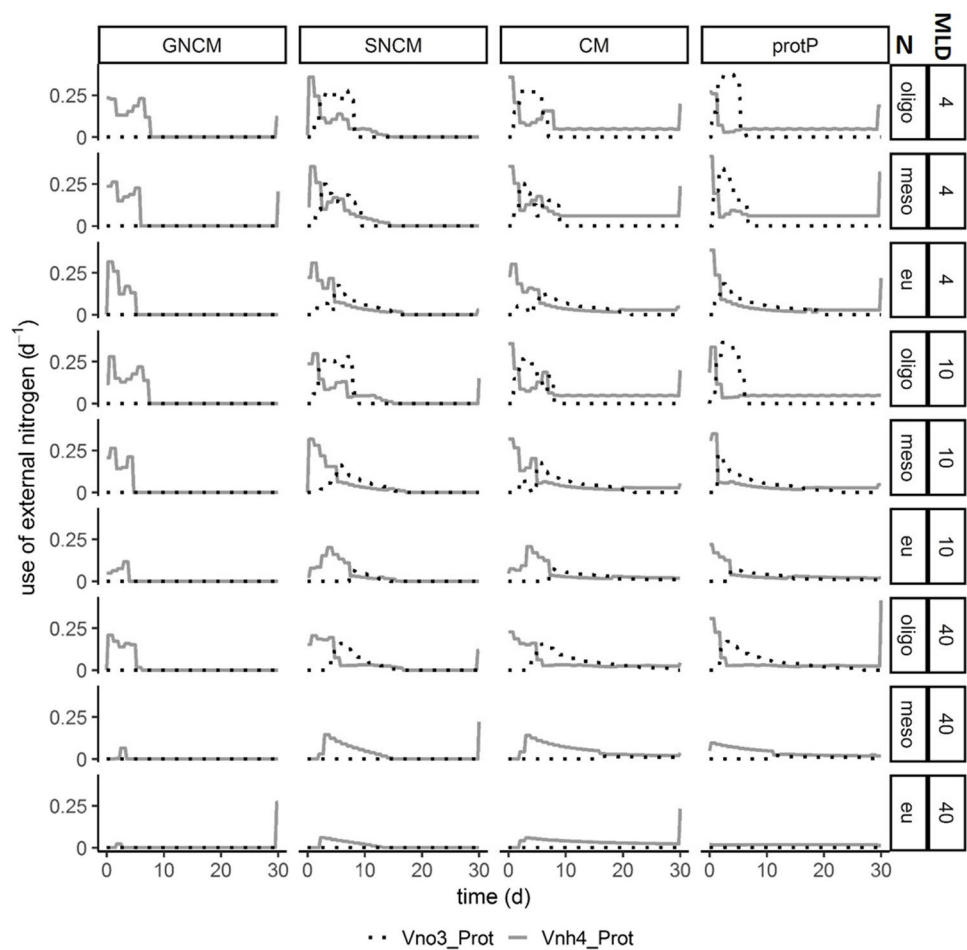
Fig. 9 Variation in the NCM
prey ingestion index (*PiI*) for
the simulations shown in Fig. 6.
These indicate that the avail-
ability of prey which thence
limits the potential for acquired
phototrophy remains greater in
low nutrient-loaded systems.
Although these are similar for
GNCM and SNCM, the impact
is much greater for the GNCM
as these need to acquire plastids
with greater frequency (see
Fig. 6). Nutrient load (oligo-,
meso- and eutrophic, Elec-
tronic Supplementary Material
Table S1) also has an effect on
the slope of the *PiI* decline in
the SNCM, because nutrient
availability impacts the expira-
tion period of the acquired chlo-
roplasts. Rows give the *MLD* (4,
10 and 40 m)
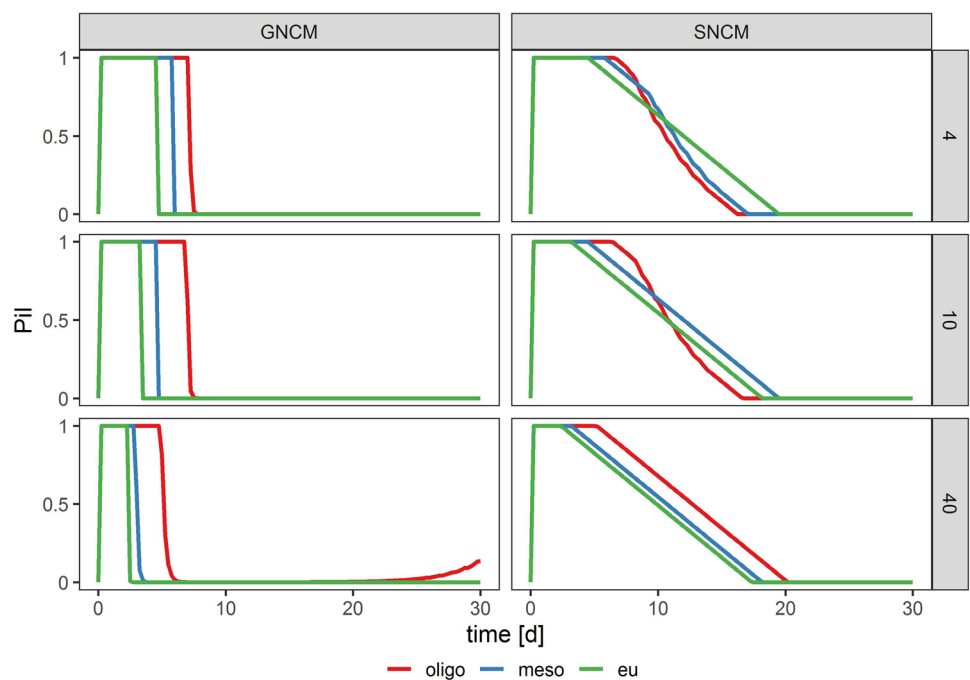
stoichiometry (C:N:P:Chl) like the perfect beast (Flynn and Mitra 2009) as implemented by Leles et al. (2018).

Ecological and biogeochemical implications

An important difference between a system containing protoZ and protP, rather than one dominated by mixoplankton as the grazer, is that growth of protoZ is inevitably associated with ammonium regeneration which supports further growth of the phototrophic prey. In contrast, mixoplankton can internalise ammonium regeneration during photosynthesis (noting that often mixoplankton predation appears to be phased to be concurrent with photosynthesis (Caron et al. 1993; Strom 2001; Brutemark and Granéli 2011; Izaguirre et al. 2012; Arias et al. 2017). If we consider such activity from the perspective of new vs regenerated production (Dugdale and Goering 1967), a nitrate-supported protP bloom would see new nitrogen supporting not only their primary production but also subsequently the primary production of predatory mixoplankton further supported by incorporation of protP-N that is internally regenerated and re-assimilated within the mixoplankton. In the simulations (which had a fixed input ratio of ammonium:nitrate), high *f*-ratios are seen mainly with the protist configured as protP or CM, and was highest in oligotrophic conditions, where organisms have to tap into the nitrate pool (Supplemental Material Fig. S8). If the growth phase of the SNCM was longer after its prey were eliminated, then the SNCM also contributes to new production. In contrast, despite their photosynthetic activity, GNCMs as described here do not directly contribute to 'new' production, because they do not use nitrate. It is not clear how important the consumption of nitrate for GNCMs is (Schoener and McManus 2017), ultimately measurements of nitrate reductase activity are required to prove such an ability. However, it is perhaps likely, given that GNCMs need to feed frequently and will thus be regenerating and recycling ammonium, that any ability to use nitrate would be minimal in any case. This is because sufficient internal ammonium would provide for the repression of nitrate and nitrite reductases and of nitrate transport (Syrett 1981; Solomonson and Barber 1990; Flynn et al. 1997).

The higher the nutrient load, the higher the biomass yield. In such situations, the CM was the most successful variant in terms of biomass yield, closely followed by the SNCM (Fig. 6). Their success is attributed to the ability to remove their competition when resources for photosynthesis (nutrients, light) become limiting. While the protP is an equal competitor to the algae in the simulation, it cannot remove its competition. When the nutrient load is too high, light becomes more attenuated due to the presence of photo-pigment carrying organisms in the water. As a result, purely phototrophic organisms cannot make as much use of the overabundant nutrients. In this context, CMs have a clear

potential for more likely forming uni-species blooms, perhaps forming HABs or EDABs (ecosystem disruptive algae bloom; Mitra and Flynn 2006). Flynn and Hansen (2013) explored the dynamics of the end of NCM blooms, noting the potential of the NCMs to continue photosynthesising as their photosystems degraded as the community Chl concentration decreased so relieving self-shading.

GNCMs and SNCMs are more limited by prey ingestion than are the CMs, as predation provides them with their photosystems. However, this same prey ingestion provides them with combined source of nutrition that also means that they are less likely to be directly limited (stressed) by inorganic nutrient availability. From the standpoint of ecological stoichiometry (Mitra and Flynn 2005; Meunier et al. 2013; Thingstad et al. 2014) this may be expected to render the NCMs as good quality prey for other trophic levels. Indeed, NCM ciliates do appear to provide good feed for higher trophic levels (Bils et al. 2017; Stoecker and Lavrentyev 2018; Zingel et al. 2019), though whether this reflects a higher visibility to predators such as fish larvae rather than a nutritional factor is not clear.

Growth of both CM and protP is more likely to be limited by external nutrient availability as they can build their own chloroplasts from scratch. However, nutrient availability for protP is dissolved inorganic while for CM this is augmented by prey nutrient. Accordingly, in the simulations the protP show signs of nutrient limitation from early in the simulations, while the CM later exploits the DIN acquired initially by the Alg1 and Alg2 and then ingested by phagotrophy (Fig. 6). CMs are not only likely to give the largest terminal bloom sizes, but those species that are toxic when nutrient stressed can form HABs (Granéli and Flynn 2006) as they exhibit high levels of variability in their stoichiometry.

Niche separation between protist types

Exploring the simulation behaviour shows that mixoplankton not only behave differently from classical phytoplankton and NPZ models, but also that there is a distinctive variation among different forms of mixoplankton (Fig. 1). A key question revolves around niche separation between the protist types: under what conditions would one or other variant be at best advantage? Not only does the mixoplankton configuration affect steady-state niche competition (Figs. 3, 4, 5), but it affects the temporal dynamics (Fig. 6). The plots shown in Figs. 3, 4, 5 show how the different protist variants provide for quite different response curves relating light and prey abundance to protist growth rate. These are all assuming all other features of physiology are held constant, that only the different selected functions are operational. In reality this is not so. For example, GNCMs are ciliates which have very different escape responses from predators than do non-ciliates. There are also differences in size ranges (Flynn

et al. 2019) with CMs typically being smaller. More fundamentally, mixoplankton grow in mature ecosystems (typified by the temperate summer), while non-mixoplankton can exploit immature systems (typified by temperate spring bloom conditions). Organisms evolve to match the supply of resources (Flynn 2009), so (mixo)plankton growing in mature systems will inevitably have lower maximum growth rates. Set against these caveats, below we compare configurations assuming that indeed all else is equal.

protoZ and protP

Microzooplankton (protoZ) display a fast "boom-and-bust" dynamic, with their growth rapidly depleting the prey and then the protoZ quickly died through starvation. The consequences are that subsequent blooms of algal prey and protoZ are also large dynamic events. In higher nutrient-loaded systems, these boom-and-bust cycles are further exaggerated. What protoZ have as an advantage over their mixoplankton counterparts is that they are not constrained by the need for photosynthesis (Hansen et al. 2013). Most mixoplankton appear to be capable of only survival in darkness (Caron et al. 1993; Kim et al. 2008; Brutemark and Granéli 2011; Hansen 2011; Hansen et al. 2013), presumably because they need some products of photosynthesis for active growth.

The protP (phytoplankton) can only compete with the algae for nutrients and light, but exert no grazing impact on them. In the model, protP thus does not exert any control over its competition, as does CM. In reality, allelopathy has the potential to reshape community structure (Granéli et al. 2008a, b). The protP only compete equally with CMs where there are insufficient prey, or for protP species that have evolved cell cycles that can be uncoupled from the diel light–dark cycle (Nelson and Brand 1979), where maximum growth rates are higher. Importantly this applies to protP as diatoms, which are also structurally highly robust and grow well in turbulent waters, while those same water conditions inhibit the growth of flagellates (Margalef 1978; Thomas and Gibson 1990), which comprise the CMs. The other critical factor for diatom growth is, of course, the need for silicate.

GNCM and SNCM

Both GNCMs and SNCMs have an advantage over protoZ, as they are not limited to just heterotrophy and therefore not as directly affected by lower prey biomass as the protoZ. At the same time, they are ultimately both constrained by an obligatory need for phagotrophy and for phototrophy. Prey consumption by GNCM is highest during daytime (Supplemental Material Fig. S7), when the products of photosynthesis mitigate against the loss of N associated with SDA. On the contrary, however, GNCMs have a lower growth rate than the protoZ when light is limiting, because

they are slowed down by the need for some level of phototrophy (competition for nutrients with algae). Under prey limitation and in shallow water without light limitation, GNCMs may have a decided advantage over protoZ as they can compensate for low prey abundance with phototrophy as long as enough prey are available to support their chloroplast demands (Figs. 6, 9). GNCMs produce a greater biomass abundance (mgN m^{-3}) in shallow water (Fig. 6) because primary production rates are higher and so in consequence are encounter rates of prey. This effect equally applies to the protoZ, which however lacks the ability to directly exploit external inorganic nitrogen.

The SNCM variant has two advantages over the GNCM.

1. It needs to ingest prey much less frequently making it more independent of the biomass of its prey; this is of most importance at low prey abundance (Fig. 4) but critically assumes that the prey that are available include the special prey that can supply photosystems (e.g. *Teleaulax*, *Mesodinium* and *Dinophysis*; Johnson and Stoecker 2005; Smith and Hansen 2007; Park et al. 2008; Nielsen et al. 2012). However, because of the ability of SNCMs to continue grazing and photosynthesising for some time after the source of their acquired phototrophy (here, Alg1) has been all but eliminated, the SNCM scenarios do not have a second bloom (Fig. 6) as the population size of Alg1 is grazed so low that it is too small to recover. The dynamics of an SNCM bloom thus requires the presence of sufficient special prey, and the very success of the SNCM bloom can be its undoing when the collective grazing on that special prey effectively eliminates it. We can thus expect that blooms of the CM *Teleaulax*, SNCM ciliate *Mesodinium* and the SNCM dinoflagellate *Dinophysis* (Minnhagen et al. 2011; Anderson et al. 2012; Reguera et al. 2012) will show a complex linkage to temporal physico-chemical ecology dynamics. With an ability to last a long time between photosystem acquisition, prey and SNCM may not even need to bloom simultaneously if the SNCM has obtained its chloroplasts from a prey bloom many weeks earlier. The SNCM receive its chloroplasts during the prey bloom and then bloom later when conditions that are favourable for it to bloom. This type of information may be highly relevant for ecosystem models driving at the prediction of harmful algae blooms caused by SNCMs like *Dinophysis*. The linkage between GNCM and its prey is much more closely matched in this context, with the need for frequent chloroplast acquisition acting to prevent a situation where the prey are eliminated. So, while on initial inspection one may think that the SNCM are advantaged by only needing to occasionally top up with acquired photosystems, the simulations

show that this may not actually contribute to an ability to form repeat blooms (Figs. 6 and 9).

2. SNCMs can use nitrate granting them access to an additional source of nitrogen (Fig. 1, 2, 6, 8). This ability gives the SNCM an edge over the GNCM especially under oligotrophic conditions, but only under conditions of good light. The ability to use nitrate may be acquired at the same time they acquire their phototrophic potential from their prey. If it is an inherent ability, reduction of nitrate to usable ammonium requires both the enzymes nitrate and nitrite reductase plus significant reductant. An advantage of the ability to use nitrate needs to be weighed against the biochemical costs (see Syrett 1981; Solomonson and Barber 1990; Fauré et al. 1991); if their prey are already using the nitrate then the cost and dangers of operating that biochemistry are borne by the prey, to the benefit of the NCM.

Feeding frequency is highly dependent on the NCMs ability to maintain the chloroplasts. In the simulation, the GNCM needs to ingest one prey cell minimum per day to receive its required chloroplasts, whereas the SNCM only needs to feed once every 30 days. The consequential impact upon growth dynamics differs between these functional types in different environmental conditions, as seen by difference in the prey ingestion index (*PiI*; Fig. 9). These critical feeding rates can be readily altered in the model by adjustment of the maximum period of time between the ingestion of one prey cell per predator (*Crit_IR*). The maximum photosynthetic rate of the GNCM is also dependent on the nutrient status of the prey from which they acquire chloroplasts, because they cannot repair them. In the GNCM variant, characteristics of the photosystem of the prey are inherited from the prey, while the SNCM variant has its own photosynthesis parameters *(maxGPS, alpha, ChlC)*. SNCMs that use the prey nucleus alongside the ingested chloroplast and are proven to have some innate genetic information for chloroplast maintenance of certain prey species will have to acquire new chloroplasts at a much lower rate than a GNCM that cannot repair any damages to the chloroplasts caused by photooxidation for example or prevent damage via photoregulation (Hansen et al. 2016).

While the SNCM ciliate *Mesodinium* reportedly needs to ingest a minimum of one specific prey cell per day to maintain maximum growth rate, it can survive up to 50 days without ingesting any of its special prey, the CM cryptophyte *Teleaulax*, at all (Smith and Hansen 2007). In fact, *Mesodinium* may feed so infrequently, that it was long believed to be a normal autotrophic phytoplankton (Olli 1999; Johnson et al. 2006), which in our model would be described as a protP. Then, it was discovered that they had to steal their chloroplasts from cryptophytes (Gustafson et al. 2000). The ability for kleptochloroplast maintenance lowers the need for frequent

ingestion and a recent study even reported division of kleptochloroplasts in *Dinophysis* spp. (Rusterholz et al. 2017). Photoacclimation, as proven in *Mesodinium* (Moeller et al. 2011), also decreases photo-oxidative stress on chloroplasts and makes them last longer.

CM

The CM configuration appears the most successful variant in all scenarios. It yields the most biomass and maintains growth much longer than other protist variants. The only exception is in shallow oligotrophic water, where the SNCM attains an equally high biomass yield for as long as suitable prey are available to provide plastids.

The CM yields the most biomass because it is not dependent on access to photosynthetic prey but can supplement its own photosynthesis by ingestion. It can therefore not only outcompete the algae for nutrients, but also remove its algal competitors that cause shading under low light conditions by resorting to phagotrophy. Once nutrients and prey are removed, the population of the CM does not collapse because it does not starve and can exploit diverse nutrient options. What makes the CM so successful is that it can eat its competition and still keep growing after its prey is depleted, because it does not rely on it to provide for acquired phototrophy (as do the NCMs). This raises the question as to why CMs are not dominant everywhere all the time. For that, we need to consider conditions required for these organisms to thrive, and those critically exclude highly turbulent systems (Margalef 1978; Thomas and Gibson 1990). Those conditions favour diatoms, which coincidentally have decoupled their cell cycle from the diel cycle, replaced a C-wall with one made of Si, and also have evolved such that they cannot engage in phagotrophy. There is thus a sharp differential between protP such as diatoms and the CMs, as described by Margalef's mandala (Margalef 1978). Between CMs and SNCMs, competitive advantage is also related to the types of organism; CMs are flagellates, while some plastidic SNCMs are flagellates, and others are ciliates.

There are various reasons why mixotrophs do not dominate in all waters, related to fragility of motile forms, a lack of prey (physiological traits that are not used are more likely lost by evolution), differences in prey–predator selections and dependencies (especially for NCMs), and differences in maximum growth rates (which are functions of system maturity, as mentioned above; Flynn 2009).

Further model development

This is a simple single nutrient (N)-based construct describing mixoplankton using two state variables; it contrasts greatly with the variable stoichiometric "perfect beast" construct of Flynn and Mitra (2009). Inevitably, the lack

of variable stoichiometry places limitations on deployment of the model we describe in this work; that is especially so when considering issues linked with ecological stoichiometry. Aside from that, the most obvious feature of protist plankton that is missing, and that has scope for profound effects on plankton dynamics, is the formation of resting stages.

Resting stages are particularly important in boom-and-bust plankton systems but are rarely considered in models. In our model, protoZ and both GNCMs and SNCMs begin to die once their growth rate falls below a certain level (Caron et al. 1990). Many GNCMs and SNCMs (e.g. *Dinophyceae*) are known to form resting cysts when conditions become unfavourable (Berland et al. 1995; Balkis et al. 2016). These cysts sink to the sediment but blooms can rapidly form from these cysts once conditions improve again (Balkis et al. 2016). Many cyst-forming organisms are also associated with harmful algae blooms (Reguera et al. 2012; Balkis et al. 2016). Cysts are also important life cycle components for CMs, such as the HAB-forming *Prymnesium parvum* and *Karlodinium micrum* (Faure et al. 2019) as well as many groups of protP, such as diatoms (Hallegraeff and Bolch 1992; McQuoid and Hobson 1996; Cremer et al. 2007). In addition, while largely inactive some of these cysts in for example *Alexandrium tamarense* are known to affect their environment by their toxicity (Oshima et al. 1992). We will explore variable stoichiometry and the dynamics of resting stages in mixoplankton growth dynamics in future works.

Compliance with ethical standards

Conflict of interest Author Anschütz declares that she has no conflict of interest. Author Flynn declares that he has no conflict of interest.

Human or animal rights This article does not contain any studies with animals performed by any of the authors.

References

Anderson DM, Cembella A, Hallegraeff GM (2012) Progress in understanding harmful algal blooms (HABs): paradigm shifts and new technologies for research, monitoring and management. Ann Rev Mar Sci 4:143–176. https://doi.org/10.1146/annurev-marine-120308-081121

Arias A, Saiz E, Calbet A (2017) Diel feeding rhythms in marine microzooplankton: effects of prey concentration, prey condition, and grazer nutritional history. Mar Biol 164:205. https://doi.org/10.1007/s00227-017-3233-7

Balkis N, Balci M, Giannakourou A, Venetsanopoulou A, Mudie P (2016) Dinoflagellate resting cysts in recent marine sediments from the Gulf of Gemlik (Marmara Sea, Turkey) and seasonal harmful algal blooms. Phycologia 55:187–209. https://doi.org/10.2216/15-93.1

Berge T, Chakraborty S, Hansen PJ, Andersen KH (2017) Modeling succession of key resource-harvesting traits of mixotrophic plankton. ISME J 11:212–223. https://doi.org/10.1038/ismej.2016.92

Berland BR, Maestrini SY, Grzebyk D (1995) Observation on possible life cycle stages of the dinoflagellates *Dinophysis cf. acuminata*, *Dinophysis acuta* and *Dinophysis pavillardi*. Aquat Microb Ecol 9:183–189

Bils F, Moyano M, Aberle N, Hufnagl M, Alvarez-Fernandez S, Peck MA (2017) Exploring the microzooplankton- ichthyoplankton link: a combined field and modeling study of Atlantic herring (*Clupea harengus*) in the Irish sea. J Plankton Res 39:147–163. https://doi.org/10.1093/plankt/fbw074

Brutemark A, Granéli E (2011) Role of mixotrophy and light for growth and survival of the toxic haptophyte *Prymnesium parvum*. Harmful Algae 10:388–394. https://doi.org/10.1016/j.hal.2011.01.005

Calbet A, Martínez RA, Isari S, Zervoudaki S, Nejstgaard JC, Pitta P, Sazhin AF, Sousoni D, Gomes A, Berger SA, Tsagaraki TM, Ptacnik R (2012) Effects of light availability on mixotrophy and microzooplankton grazing in an oligotrophic plankton food web: evidences from a mesocosm study in Eastern Mediterranean waters. J Exp Mar Biol Ecol 424–425:66–77. https://doi.org/10.1016/j.jembe.2012.05.005

Caron DA, Goldman A, Fenchel T (1990) Protozoan respiration and metabolism. In: Capriulo GM (ed) Ecology of marine protozoa. Oxford University Press, New York, pp 307–322

Caron DA, Sanders RW, Lim EL, Marrasé C, Amaral LA, Whitney S, Aoki RB, Porters KG (1993) Light-dependent phagotrophy in the freshwater mixotrophic chrysophyte *Dinobryon cylindricum*. Microb Ecol 25:93–111. https://doi.org/10.1007/BF00182132

Cremer H, Sangiorgi F, Wagner-Cremer F, McGee V, Lotter AF, Visscher H (2007) Diatoms (Bacillariophyceae) and Dinoflagellate Cysts (Dinophyceae). Caribb J Sci 43:23–58. https://doi.org/10.1007/s11116-014-9521-x

Dolan JR, Pérez MT (2000) Costs, benefits and characteristics of mixotrophy in marine oligotrichs. Freshw Biol 45:227–238. https://doi.org/10.1046/j.1365-2427.2000.00659.x

Dugdale RC, Goering JJ (1967) Uptake of new and regenerated forms of nitrogen in primary productivity. Limnol Oceanogr 12:196–206. https://doi.org/10.4319/lo.1967.12.2.0196

Fasham MJR, Ducklow HW, McKelvie SM (1990) A nitrogen-based model of plankton dynamics in the oceanic mixed layer. J Mar Res 48:591–639. https://doi.org/10.1357/002224090784984678

Faure E, Not F, Benoiston A-S, Labadie K, Bittner L, Ayata S-D (2019) Mixotrophic protists display contrasted biogeographies in the global ocean. ISME J. https://doi.org/10.1038/s41396-018-0340-5

Fauré J, Vincentz M, Kronenberger J, Caboche M (1991) Co- regulated expression of nitrate and nitrite reductases. Fedn eur Biochem Soc Lett 392:1–5

Flynn KJ (2009) Going for the slow burn: why should possession of a low maximum growth rate be advantageous for microalgae? Plant Ecol Divers 2:179–189. https://doi.org/10.1080/17550870903207268

Flynn KJ (2018) Dynamic ecology—an introduction to the art of simulating trophic dynamics. Swansea University, Swansea. ISBN 978-0-9567462-9-0

Flynn KJ, Hansen PJ (2013) Cutting the canopy to defeat the "Selfish Gene"; conflicting selection pressures for the integration of phototrophy in mixotrophic protists. Protist 164:1–13. https://doi.org/10.1016/j.protis.2013.09.002

Flynn KJ, Mitra A (2009) Building the "perfect beast": modelling mixotrophic plankton. J Plankton Res 31:965–992. https://doi.org/10.1093/plankt/fbp044

Flynn KJ, Mitra A (2016) Why plankton modelers should reconsider using rectangular hyperbolic (Michaelis-Menten, Monod) descriptions of predator-prey interactions. Front Mar Sci. https://doi.org/10.3389/fmars.2016.00165

Flynn KJ, Fasham MJR, Hipkin CR (1997) Modelling the interactions between ammonium and nitrate uptake in marine phytoplankton. Philos Trans R Soc B 352:1625–1645

Flynn KJ, Stoecker DK, Mitra A, Raven JA, Glibert PM, Hansen PJ, Granéli E, Burkholder JM (2013) Misuse of the phytoplankton–zooplankton dichotomy: the need to assign organisms as mixotrophs within plankton functional types. J Plankton Res 35:3–11. https://doi.org/10.1093/plankt/fbs062

Flynn KJ, Mitra A, Anestis K, Anschütz AA, Calbet A, Ferreira GD, Gypens N, Hansen PJ, John U, Martin JL, Mansour JS, Maselli M, Medić N, Norlin A, Not F, Pitta P, Romano F, Saiz E, Schneider LK, Stolte W, Traboni C (2019) Mixotrophic protists and a new paradigm for marine ecology: where does plankton research go now? J Plankton Res. https://doi.org/10.1093/plankt/fbz026

Franks PJS (2002) NPZ models of plankton dynamics: their construction, coupling to physics, and application. J Oceanogr 58:379–387. https://doi.org/10.1023/A:1015874028196

Granéli E, Flynn KJ (2006) Chemical and physical factors influencing toxin production. In: Granéli E, Turner JT (eds) Ecology of harmful algae, ecological. Springer, Berlin, pp 229–241

Granéli E, Weberg M, Salomon PS (2008a) Harmful algal blooms of allelopathic microalgal species: the role of eutrophication. Harmful Algae 8:94–102. https://doi.org/10.1016/j.hal.2008.08.011

Granéli E, Salomon PS, Fistarol GO (2008b) The role of allelopathy for harmful algae bloom formation. Algal toxins: nature, occurrence, effect and detection. Springer, New York, pp 159–178

Gustafson DE, Stoecker DK, Johnson MD, Van Heukelem WF, Sneider K (2000) Cryptophyte algae are robbed of their organelles by the marine ciliate *Mesodinium rubrum*. Nature 405:1049–1052. https://doi.org/10.1177/0956247816647344

Hallegraeff GM, Bolch CJ (1992) Transport of diatom and dinoflagellate resting spores in ships' ballast water: implications for plankton biogeography and aquaculture. J Plankton Res 14:1067–1084

Hammer AC, Pitchford JW (2005) The role of mixotrophy in plankton bloom dynamics, and the consequences for productivity. ICES J Mar Sci 62:833–840. https://doi.org/10.1016/j.icesjms.2005.03.001

Hansen PJ (2011) The role of photosynthesis and food uptake for the growth of marine mixotrophic dinoflagellates. J Eukaryot Microbiol 58:203–214. https://doi.org/10.1111/j.1550-7408.2011.00537.x

Hansen PJ, Nielsen LT, Johnson M, Berge T, Flynn KJ (2013) Acquired phototrophy in *Mesodinium* and *Dinophysis*—a review of cellular organization, prey selectivity, nutrient uptake and bioenergetics. Harmful Algae 28:126–139. https://doi.org/10.1016/j.hal.2013.06.004

Hansen PJ, Ojamäe K, Berge T, Trampe ECL, Nielsen LT, Lips I, Kühl M (2016) Photoregulation in a kleptochloroplastidic dinoflagellate, *Dinophysis acuta*. Front Microbiol. https://doi.org/10.3389/fmicb.2016.00785

Izaguirre I, Sinistro R, Schiaffino MR, Sánchez ML, Unrein F, Massana R (2012) Grazing rates of protists in wetlands under contrasting light conditions due to floating plants. Aquat Microb Ecol 65:221–232. https://doi.org/10.3354/ame01547

Jacobson D, Andersen R (1994) Dinophysis (Dinophyceae): light and electron microscopical observations of food vacuoles in *Dinophysis acuminata*, *D. norvegica* and two heterotrophic dinophysoid. Phycologia 33:97–110

Johnson MD, Stoecker DK (2005) Role of feeding in growth and photophysiology of *Myrionecta rubra*. Aquat Microb Ecol 39:303–312. https://doi.org/10.3354/ame039303

Johnson MD, Tengs T, Oldach D, Stoecker DK (2006) Sequestration, performance, and functional control of cryptophyte plastids in the ciliate *Myrionecta rubra* (ciliophora). J Phycol 42:1235–1246. https://doi.org/10.1111/j.1529-8817.2006.00275.x

Johnson MD, Oldach D, Delwiche CF, Stoecker DK (2007) Retention of transcriptionally active cryptophyte nuclei by the ciliate *Myrionecta rubra*. Nature 445:426–428. https://doi.org/10.1038/nature05496

Kenny P, Flynn KJ (2016) Coupling a simple irradiance description to a mechanistic growth model to predict algal production in industrial-scale solar-powered photobioreactors. J Appl Phycol 28:3203–3212. https://doi.org/10.1007/s10811-016-0892-6

Kim S, Kang YG, Kim HS, Yih W, Coats DW, Park MG (2008) Growth and grazing responses of the mixotrophic dinoflagellate *Dinophysis acuminata* as functions of light intensity and prey concentration. Aquat Microb Ecol 51:301–310. https://doi.org/10.3354/ame01203

Leles SG, Mitra A, Flynn KJ, Stoecker DK, Hansen PJ, Calbet A, McManus GB, Sanders RW, Caron DA, Not F, Hallegraeff GM, Pitta P, Raven JA, Johnson MD, Glibert PM, Våge S (2017) Oceanic protists with different forms of acquired phototrophy display contrasting biogeographies and abundance. Proc R Soc B Biol Sci 284:20170664. https://doi.org/10.1098/rspb.2017.0664

Leles SG, Polimene L, Bruggeman J, Blackford J, Ciavatta S, Mitra A, Flynn KJ (2018) Modelling mixotrophic functional diversity and implications for ecosystem function. J Plankton Res 40:627–642. https://doi.org/10.1093/plankt/fby044

Leles SG, Mitra A, Flynn KJ, Tillmann U, Stoecker D, Jeong HJ, Burkholder JA, Hansen PJ, Caron DA, Glibert PM, Hallegraeff G, Raven JA, Sanders RW, Zubkov M (2019) Sampling bias misrepresents the biogeographical significance of constitutive mixotrophs across global oceans. Glob Ecol Biogeogr 28:418–428. https://doi.org/10.1111/geb.12853

Margalef R (1978) Life-forms of phytoplankton as survival alternatives in an unstable environment. Oceanol Acta 1:493–509

McManus GB, Zhang H, Lin S (2004) Marine planktonic ciliates that prey on macroalgae and enslave their chloroplasts. Limnol Oceanogr 49:308–313. https://doi.org/10.4319/lo.2004.49.1.0308

McQuoid MR, Hobson LA (1996) Diatom resting stages. J Phycol 32:889–902. https://doi.org/10.1080/01418619108213945

Meunier CL, Schulz K, Boersma M, Malzahn AM (2013) Impact of swimming behaviour and nutrient limitation on predator-prey interactions in pelagic microbial food webs. J Exp Mar Bio Ecol 446:29–35. https://doi.org/10.1016/j.jembe.2013.04.015

Minnhagen S, Kim M, Salomon PS, Yih W, Granéli E, Park MG (2011) Active uptake of kleptoplastids by *Dinophysis caudata* from its ciliate prey *Myrionecta rubra*. Aquat Microb Ecol 62:99–108. https://doi.org/10.3354/ame01459

Mitra A, Flynn KJ (2005) Predator-prey interactions: Is "ecological stoichiometry" sufficient when good food goes bad? J Plankton Res 27:393–399. https://doi.org/10.1093/plankt/fbi022

Mitra A, Flynn KJ (2006) Promotion of harmful algal blooms by zooplankton predatory activity. Biol Lett 2:194–197. https://doi.org/10.1098/rsbl.2006.0447

Mitra A, Flynn KJ (2010) Modelling mixotrophy in harmful algal blooms: more or less the sum of the parts? J Mar Syst 83:158–169. https://doi.org/10.1016/j.jmarsys.2010.04.006

Mitra A, Flynn KJ, Tillmann U, Raven JA, Caron D, Stoecker DK, Not F, Hansen PJ, Hallegraeff G, Sanders R, Wilken S, McManus G, Johnson M, Pitta P, Våge S, Berge T, Calbet A, Thingstad F, Jin H, Burkholder JA, Glibert PM, Granéli E, Lundgren V, Jeong HJ, Burkholder JA, Glibert PM, Granéli E, Lundgren V, Jin H, Burkholder JA, Glibert PM, Granéli E, Lundgren V, Jeong HJ, Burkholder JA, Glibert PM, Granéli E, Lundgren V (2016) Defining planktonic protist functional groups on mechanisms for energy and nutrient acquisition: incorporation of diverse mixotrophic strategies. Protist 167:106–120. https://doi.org/10.1016/j.protis.2016.01.003

Moeller HV, Johnson MD, Falkowski PG (2011) Photoacclimation in the phototrophic marine ciliate *Mesodinium rubrum* (ciliophora). J Phycol 47:324–332. https://doi.org/10.1111/j.1529-8817.2010.00954.x

Nelson DM, Brand LE (1979) Cell division periodicity in 13 species of marine phytoplankton on a light:dark cycle. J Phycol 15:67–75

Nielsen LT, Krock B, Hansen PJ (2012) Effects of light and food availability on toxin production, growth and photosynthesis in *Dinophysis acuminata*. Mar Ecol Prog Ser 471:37–50. https://doi.org/10.3354/meps10027

Olli K (1999) Diel vertical migration of phytoplankton and heterotrophic flagellates in the Gulf of Riga. J Mar Syst 23:145–163. https://doi.org/10.1016/S0924-7963(99)00055-X

Oshima Y, Bolch CJ, Hallegraeff GM (1992) Toxin composition of resting cysts of *Alexandrium tamarense* (Dinophyceae). Toxicon 30:1539–1544

Park MG, Park JS, Kim M, Yih W (2008) Plastid dynamics during survival of *Dinophysis caudata* without its ciliate prey. J Phycol 44:1154–1163. https://doi.org/10.1111/j.1529-8817.2008.00579.x

Pitta P, Giannakourou A, Christaki U (2001) Planktonic ciliates in the oligotrophic Mediterranean Sea: longitudinal trends of standing stocks, distributions and analysis of food vacuole contents. Aquat Microb Ecol 24:297–311. https://doi.org/10.3354/ame024297

Reguera B, Velo-Suárez L, Raine R, Park MG (2012) Harmful *Dinophysis* species: a review. Harmful Algae 14:87–106. https://doi.org/10.1016/j.hal.2011.10.016

Rothschild BJ, Osborn TR (1988) Small-scale turbulence and plankton contact rates. J Plankton Res 10:465–474. https://doi.org/10.1093/plankt/10.3.465

Rusterholz PM, Hansen PJ, Daugbjerg N (2017) Evolutionary transition towards permanent chloroplasts?—division of kleptochloroplasts in starved cells of two species of *Dinophysis* (Dinophyceae). PLoS One. https://doi.org/10.1371/journal.pone.0177512

Schoener DM, McManus GB (2012) Plastid retention, use, and replacement in a kleptoplastidic ciliate. Aquat Microb Ecol 67:177–187. https://doi.org/10.3354/ame01601

Schoener DM, McManus GB (2017) Growth, grazing, and inorganic C and N uptake in a mixotrophic and a heterotrophic ciliate. J Plankton Res 39:379–391. https://doi.org/10.1093/plankt/fbx014

Smith EL (1936) Photosynthesis in relation to light and carbon dioxide. Proc Natl Acad Sci 22:504–511. https://doi.org/10.1073/pnas.22.8.504

Smith M, Hansen PJ (2007) Interaction between *Mesodinium rubrum* and its prey: importance of prey concentration, irradiance and pH. Mar Ecol Prog Ser 338:61–70. https://doi.org/10.3354/meps338061

Solomonson LP, Barber MJ (1990) Assimilatory nitrate reductase: functional properties and regulation. Annu Rev Plant Biol 41:225–253

Stickney HL, Hood RR, Stoecker DK (2000) The impact of mixotrophy on planktonic marine ecosystems. Ecol Modell 125:203–230

Stoecker DK, Lavrentyev PJ (2018) Mixotrophic plankton in the Polar Seas: a Pan-Arctic review. Front Mar Sci. https://doi.org/10.3389/fmars.2018.00292

Strom SL (2001) Light-aided digestion, grazing and growth in herbivorous protists. Aquat Microb Ecol 23:253–261. https://doi.org/10.1088/0256-307X/23/7/022

Syrett PJ (1981) Nitrogen metabolism of microalgae. In: Platt T (ed) Physiological bases of phytoplankton ecology. Canadian Government Publishing Centre, Canadian Bulletin of Fisheries and Aquatic Science, Ottawa, pp 182–210

Thingstad TF, Havskum H, Garde K, Riemann B, Ecology S, Oct N (1996) On the strategy of "Eating Your Competitor": a mathematical analysis of algal mixotrophy. Ecology 77:2108–2118. https://doi.org/10.2307/2265705

Thingstad F, Tillmann U, Våge S, Wilken S, Zubkov MV (2014) The role of mixotrophic protists in the biological carbon pump. Biogeosciences 11:995–1005. https://doi.org/10.5194/bg-11-995-2014

Thomas WH, Gibson CH (1990) Effects of small-scale turbulence on microalgae. J Appl Phycol 2:71–77

Ward BA, Dutkiewicz S, Barton AD, Follows MJ (2011) Biophysical aspects of resource acquisition and competition in algal mixotrophs. Am Nat 178:98–112. https://doi.org/10.1086/660284

Wilkerson FP, Grunseich G (1990) Formation of blooms by the symbiotic ciliate *Mesodinium rubrum*: the significance of nitrogen uptake. J Plankton Res 12:973–989

Yoo YD, Seong KA, Jeong HJ, Yih W, Rho J-R, Nam SW, Kim HS (2017) Mixotrophy in the marine red-tide cryptophyte *Teleaulax amphioxeia* and ingestion and grazing impact of cryptophytes on natural populations of bacteria in Korean coastal waters. Harmful Algae 68:105–117. https://doi.org/10.1016/j.hal.2017.07.012

Yool A, Popova EE, Anderson TR (2013) Geoscientific model development MEDUSA-2.0: an intermediate complexity biogeochemical model of the marine carbon cycle for climate change and ocean acidification studies. Geosci Model Dev 6:1767–1811. https://doi.org/10.5194/gmd-6-1767-2013

Zingel P, Agasild H, Karus K, Buholce L, Nõges T (2019) Importance of ciliates as food for fish larvae in a shallow sea bay and a large shallow lake. Eur J Protistol 67:59–70. https://doi.org/10.1016/j.ejop.2018.10.004